1970-06

An investigation of swirling flow in a convergent funnel.

Hornstra, Douglas John

Monterey, California ; Naval Postgraduate School

AN INVESTIGATION OF SWIRLING FLOW IN A CONVERGENT FUNNEL

Douglas John Hornstra

United States
Naval Postgraduate School

THESIS

AN INVESTIGATION OF
SWIRLING FLOW IN A CONVERGENT FUNNEL

by

Douglas John Hornstra

June 1970

An Investigation of Swirling Flow in a Convergent Funnel

by

Douglas John Hornstra
Lieutenant (junior grade), United States Navy
B.S., Tufts University, 1969

Submitted in partial fulfillment of the
requirements of the degree of

MASTER OF SCIENCE IN MECHANICAL ENGINEERING

from the

NAVAL POSTGRADUATE SCHOOL
June 1970

ABSTRACT

The boundary layer for a swirling flow of incompressible fluid in a convergent cone has been investigated. Theoretical calculation with boundary conditions more appropriate to physically existent situations discount the existence of "super velocities" within the boundary layer. Parallel experimental investigations demonstrate an interdependence of core and boundary layer flows which precludes the maintenance of initial "ideal flow" conditions.

TABLE OF CONTENTS

LIST OF FIGURES

NOMENCLATURE

u	velocity in x direction - axial velocity
v	velocity in θ direction - tangential velocity
w	velocity in z direction
x	distance along the wall
z	distance perpendicular to wall
K	initial ratio of tangential to axial velocities
U	free stream velocity in x direction
U'	derivative with to X of U
V	free stream tangential velocity
V'	derivative with respect to X of V
$\vec{a}$	acceleration vector
$\vec{q}$	velocity vector
ζ	vorticity
μ	viscosity
ν	kinematic viscosity
ρ	density
τ_o	shear at the wall

ACKNOWLEDGEMENTS

The author is indebted to Asst. Professor T. M. Houlihan for his invaluable assistance and encouragement. The author also wishes to thank Mr. George Bixler for his assistance in the construction of the apparatus.

I. INTRODUCTION

The determination of velocity profiles in the laminar boundary layer of a convergent nozzle has been approached analytically in several different manners. Taylor [1] considered the case of a predominant tangential flow with a secondary axial flow. In his analysis, Taylor assumed that the tangential flow exceeded the axial flow to the extent that the axial component in the inviscid core could be neglected. After applying the Pohlhausen method to the mementum-integral equations and obtaining solutions for various axial positions, Taylor concluded that a condition could arise when most of the outflow from the nozzle was fed by a boundary-layer current close to the wall of the swirl chamber. The radial pressure gradient, which held the particles in their circular path, acted upon the retarded boundary layer to drive the fluid along the surface to the exit.

Wilks [2] developed a similar approach that led to the possibility of a 'super-velocity' existing in the boundary layer of a convergent conical nozzle. This 'super-velocity' was a velocity within the boundary layer that exceeded the free-stream velocity. Wilks considered the flow in the cone to be that of an inviscid core with a thin boundary layer. The inviscid core had two components of flow - a uniform axial flow and a free vortex with its center along the center line of the nozzle.

In this paper an analogous approach was utilized. However, the effect of the boundary-layer growth upon the tangential

and axial velocities in the free stream flow was considered. Subsequently, no super-volocities were found to exist. Furthermore, experimental results prove that full scale effects predominate in this problem rather than just boundary-layer effects.

II. ANALYSES

A. WILKS THEORY

Using the Wilks approach, a curvilinear coordinate system was defined with the x-axis along the wall and the z-axis perpendicular to the wall of the nozzle (Figure in Appendix A). The shape of the nozzle was determined by the surface of revolution of an arbitrary curve r(x). Wilks developed an approximate method of solution using the momentum equations (Appendix A)

$$u \frac{\partial u}{\partial x} + w \frac{\partial u}{\partial z} - \frac{v^2 dr}{r\, dx} = U \frac{dU}{dx} - \frac{V^2 dr}{r\, dx} + \nu \frac{\partial^2 u}{\partial z^2} \tag{1}$$

$$u \frac{\partial v}{\partial x} + w \frac{\partial v}{\partial z} + \frac{uv}{r} \frac{dr}{dx} = \nu \frac{\partial^2 v}{\partial z^2} \tag{2}$$

$$\frac{\partial}{\partial x} (r \cdot u) + \frac{\partial}{\partial z} (r \cdot w) = 0 \tag{3}$$

and the corresponding integrated forms of the momentum equations

$$\frac{1}{r} \frac{d}{dx} \left(r \int_0^\infty u(u-U)\, dz\right) + \frac{dU}{dx} \int_0^\infty (u-U)\, dz + \frac{r'}{r} \int_0^\infty (V^2 - v^2)\, dz \tag{4}$$

$$= - \nu \left(\frac{\partial u}{\partial z}\right)_0$$

$$\frac{1}{r^2} \frac{d}{dx} \left(r^2 \int_0^\infty u(v-V)\, dz\right) = - \nu \left(\frac{\partial v}{\partial z}\right)_0 , \tag{5}$$

where the boundary conditions were

$$\begin{aligned} &u = 0; \quad - \nu \frac{\partial^2 u}{\partial z^2} = U \frac{dU}{dx} - V^2 \frac{r'}{r}; \quad \text{on } z = 0 \\ &u = U(x); \quad \frac{\partial u}{\partial z} = 0; \quad \frac{\partial^2 u}{\partial z^2} = 0; \quad \text{when } z \to \infty \end{aligned} \tag{6}$$

and

$$v = 0;\ \frac{\partial^2 v}{\partial z^2} = 0; \quad \text{on } z = 0$$

$$v = V(x) = \frac{A}{r(x)};\ \frac{\partial v}{\partial z} = 0;\ \frac{\partial^2 v}{\partial z^2} = 0; \quad \text{when } z \to \infty \tag{7}$$

The distances in the above equations were non-dimensionalized by defining $n = z / \delta$ and $X = x / c$, where δ was the local boundary-layer thickness and c was the distance along the generator to the nozzle to its apex.

To obtain a solution of the momentum-integral equations, it was necessary to assume a velocity profile within the boundary layer. A profile that would also satisfy the energy-integral equations should produce some improvement over a solution to the momentum-integral equation alone. Wieghardt [3] developed such a method with the use of two free parameters and an eleventh-degree polynomial. Applying the free parameters and the polynomial to the u-velocity profile and assuming that the v-velocity profile did not change significantly with X, the following profiles were obtained:

$$u/U = f_1(n) + L_1 \cdot f_2(n) + L_2 \cdot f_3(n) \tag{8}$$

where

$$f_1(n) = 1 - (1 - n)^8(1 + 8n + 36n^2 + 120n)$$

$$f_2(n) = (1 - n)^8 n(1 + 8n + 36n^2)$$

$$f_3(n) = -(1 - n)^8 n^2(1 + 8n)$$

and

$$v/V = g(n) = 2n - 2n^3 + n^4 \qquad (9)$$

An evaluation of the axial velocity profile at the wall leads to physical connotations for the shape factors, L_1 and L_2; i.e., L_1 includes the wall shear stress and L_2 involves the axial pressure gradient.

$$L_1 = \frac{\tau_o \delta}{\mu U} \qquad L_2 = \frac{\delta}{2c} \frac{\delta}{\mu U} \left(-\frac{dP}{dX}\right)$$

Using the coefficients A1, A2, A3 and A4 (ratios of characteristic thicknesses) as defined in APPENDIX A and introducing a term

$$G = \left(\frac{U\delta}{\nu}\right)\left(\frac{\delta}{c}\right) = \left(\frac{U\delta^2}{\nu c}\right)$$

the momentum-integral equations became

$$\frac{r'}{r} + \frac{U'}{U}(2 + A1) + \frac{\delta'_{2x}}{\delta_{2x}} = \frac{A2}{G} + \frac{r'}{r}\left(\frac{V}{U}\right)^2 A3 \qquad (10)$$

$$\frac{r'}{r} + \frac{U'}{U} + \frac{\delta'_{2xy}}{\delta_{2xy}} = \frac{A4}{G} \qquad (11)$$

As a method of simplifying the solution, Wilks assumed that a basically linear relationship existed between the momentum thickness (δ_{2x}) and the boundary-layer thickness (δ) and between the mixed momentum thickness (δ_{2xy}) and the boundary-layer thickness. The above equations were then combined with the definition of G and its derivative. The following relationships were obtained

$$G' = 2 \cdot A4 - \frac{(A2 - A4)}{(A1 - 1)} - G \frac{r'}{r} \left\{ 2 + \left(\frac{V}{U}\right)^2 \frac{A3}{(1 + A1)} \right\} \qquad (12)$$

$$A2 = G \frac{U'}{U}(1 + A1) + A4 - G \frac{r'}{r} \left(\frac{V}{U}\right)^2 A3 \qquad (13)$$

$$L_2 = \frac{G}{2} \left\{ \frac{U'}{U} - \frac{V^2}{U^2} \frac{r'}{r} \right\} \qquad (14)$$

In the preceeding analysis, no restriction was made upon the shape of the convergent nozzle. The flow conditions in a cone, as well as many other shaped nozzles, do not meet the requirements for a similarity solution of the related boundary layer equations. However, in these cases where the profiles vary with axial position in a non-linear manner, this present approximate method of solution can be universally used. Wilks showed that a solution of the similarity equation could be developed for any one point along the surface of a cone, but that the coefficients of the Falkner-Skan equation would be different for each point. For each point, he noted that a close agreement existed between the profiles of the approximate method of solution and the profiles of the similarity solution.

For the particular case of a cone, a linear relationship existed between the radius and X. The axial velocity as a functions of X was then formulated from continuity, and the variations in the tangential velocity were derived from conservation of angular momentum. (The details of these functions are given in APPENDIX A.)

B. NUMERICAL SOLUTION OF WILKS THEORY

A solution of the momentum-integral equations would lead to the values of the shape factors and thus to the axial velocity profile. A step-by-step procedure was used to solve the governing equations at various values of X. Wilks considered the simplified case where the initial boundary-layer thickness on the cone was zero. With this assumption, G(0) became zero, which led to $L_2(0) = 0$. Equation 13 then became a quadratic in $L_1(0)$. The solution for other values of X continued in the following iterative manner:

(1) Using the values of $L_1(0)$ and $L_2(0)$, the thickness coefficients were calculated.

(2) The velocities were then evaluated.

(3) Using equation 13, L_1 was calculated.

(4) Applying equation 12, the value of G' was determined.

(5) Using the first two terms of a Taylor series expansion, $G(X+dX) = G(X) + G'(X) \cdot dX$.

(6) L_2 was calculated from equation 14.

(7) The values of the thickness coefficients were recalculated with the new values of L_1 and L_2 and the procedure from step 2 onward was repeated for new values of X.

In a physical system, a boundary layer could easily exist before the flow entered the conical region. The momentum-integral equations would then need to be solved for a non-zero initial boundary-layer thickness. This was accomplished by a

slight modification of the Wilks solution. Using the solution of the quadratic in $L_1(0)$ for zero initial boundary-layer thickness as a predicted value of $L_1(0)$, an iterative method would correct this value for the presence of an initial boundary-layer thickness. The method pursued was the following:

(1) An initial value for $L_1(0)$ was assumed.

(2) The velocities were calculated.

(3) G and thus L_2 were determined from the value of the initial boundary-layer thickness.

(4) Using the current values for $L_1(0)$ and $L_2(0)$, the thickness coefficients were calculated.

(5) The value of $L_1(0)$ was determined according to equation 13.

(6) The calculated value of L_1 was compared with the assumed value of L_1. If the two values were not sufficiently close, a value equal to the average of the two was assumed and the procedure from step 4 onward was repeated. If the result was sufficiently accurate, L_1 and L_2 were calculated for other values of X using the same methods as for a zero initial boundary-layer thickness.

Using the above numerical methods, the momentum-integral equations were solved for values of K (swirl factor) of one and two. The resultant profiles were compared with the Wilks profiles to insure the correctness of the numerical method

employed. The solution was then extended for values of K up to six with various initial thicknesses and initial velocities. Several profiles that were obtained in this manner are shown in Figures 1-7. The solutions indicated that the degree of super-velocity increased dramatically with K and X. The value of the momentum thickness became negative under many circumstances, and for high degrees of super-velocity, the displacement thickness also became negative. Under all of these conditions the boundary-layer growth continued to increase with X. The numerical analysis deteriorated for values of X much greater than 0.3 in most of these solutions. There was also a failure in the numerical solution for ratios of tangential velocity to axial velocity in the range of three. It was believed that these problems were caused by the numerical method employed and were not inherent problems of the analytical model. The quantity (A2 - A4) could be very close to zero. Since one of the terms in the calculation of L_1 required division by the above quantity, overflow in the computer could easily be caused when this quantity approached zero. A different final arrangement of the momentum-integral equations would avoid this problem and allow for a solution at higher values of X.

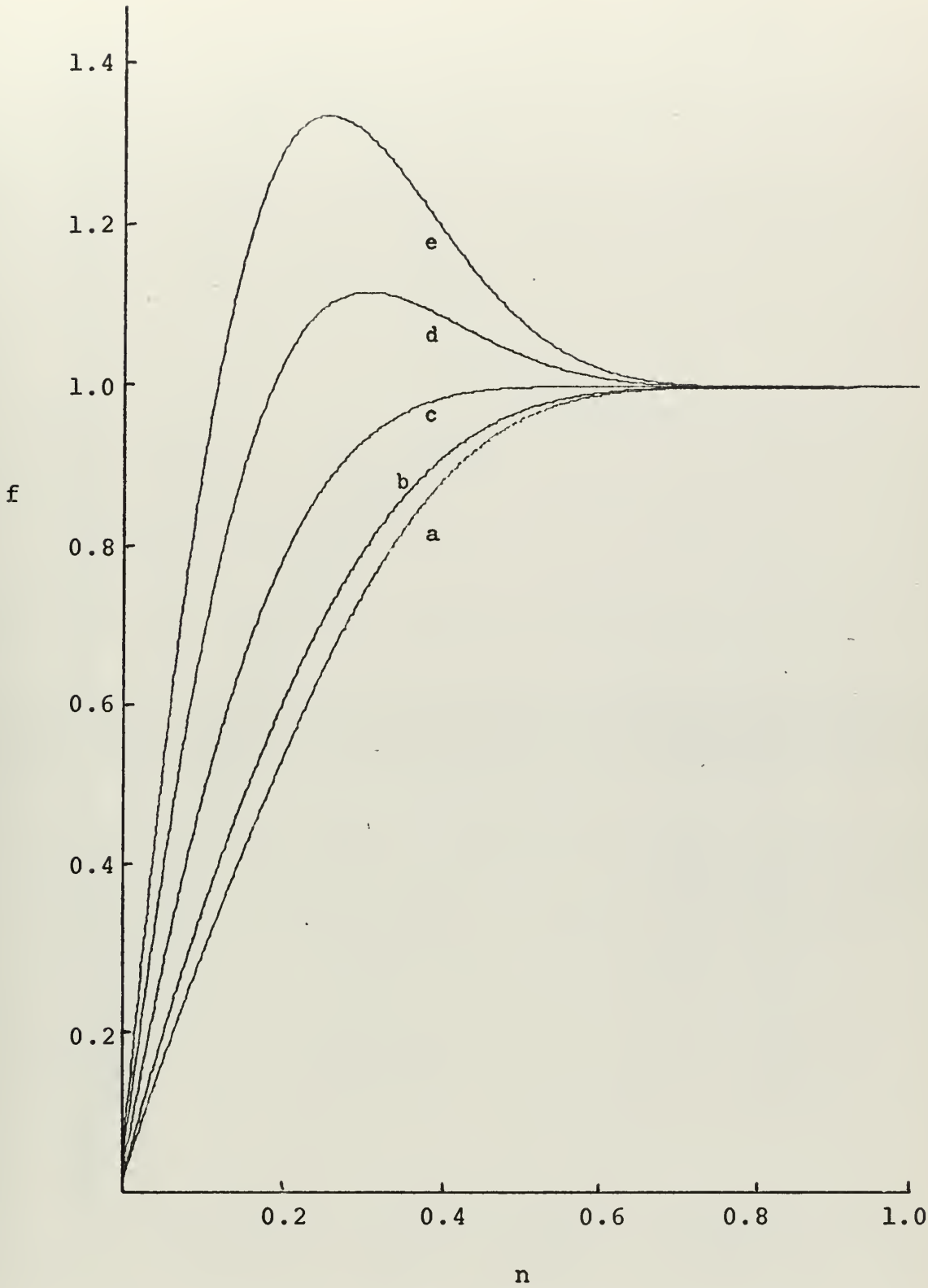

FIGURE 1. VARIATIONS IN PROFILE WITH K. X=0.1 G(0)=0

(a) K=0 , (b) K=1 , (c) K=2 , (d) K=3 , (e) K=4

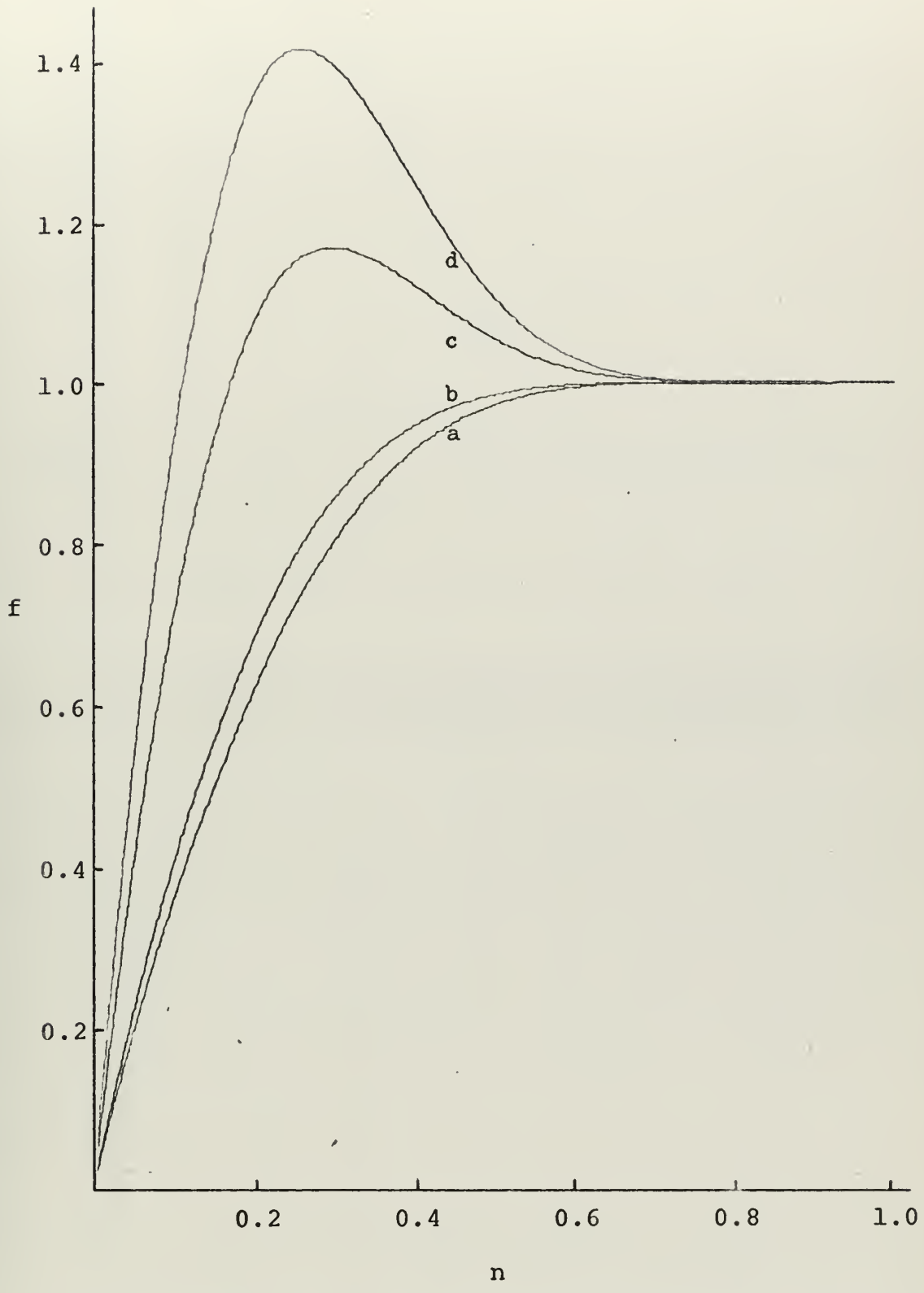

FIGURE 2. VARIATIONS IN PROFILE WITH K. X=0.1 G(0)=0.52

(a) K=1 , (b) K=2 , (c) K=3 , (d) K=4

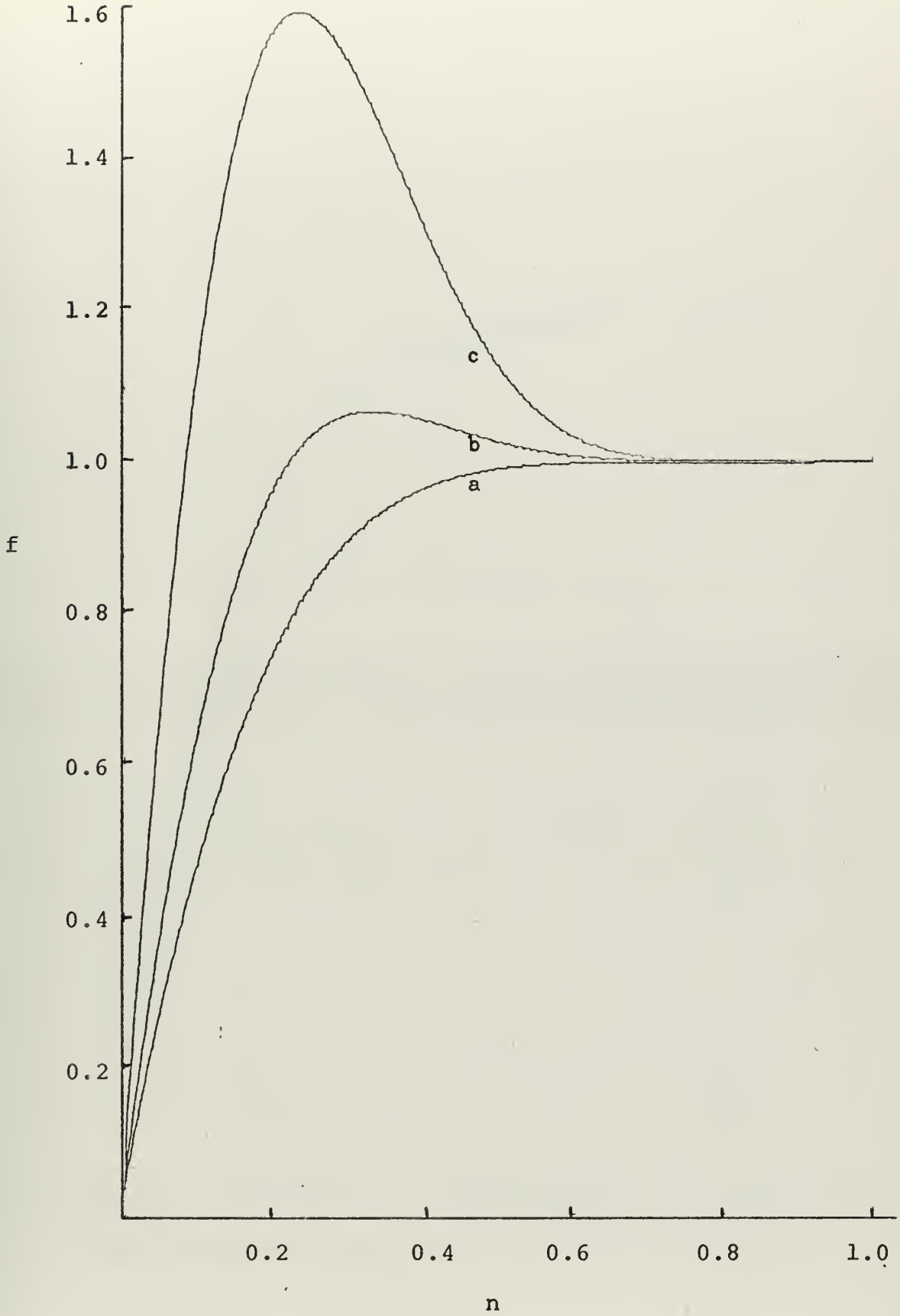

FIGURE 3. VARIATIONS IN PROFILE WITH K. X=0.2 G(0)=0.52

(a) K=1 , (b) K=2 , (c) K=4

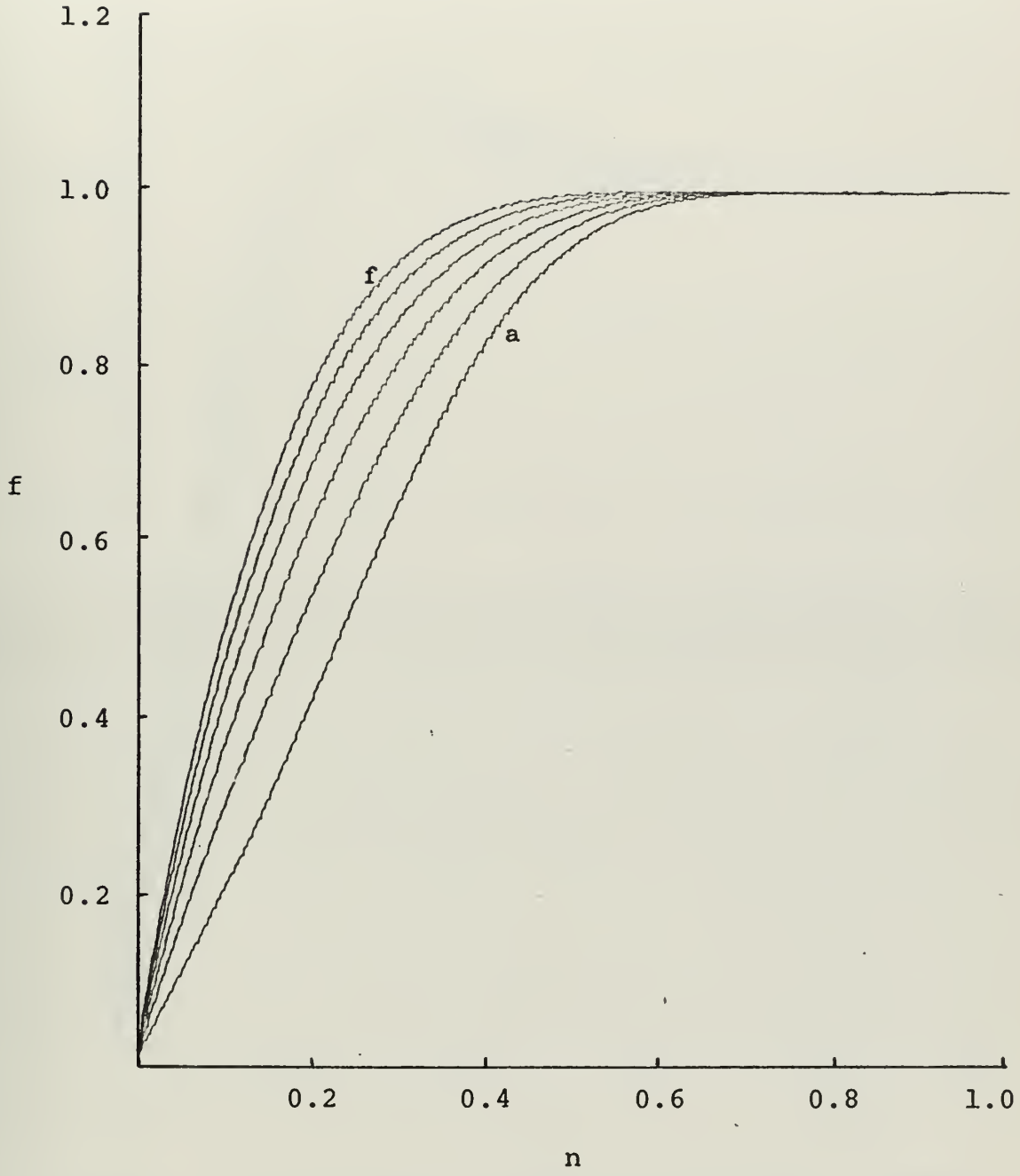

FIGURE 4. VARIATIONS IN PROFILE WITH X. K=1 G(0)=0.52

(a) X=0.00 , (b) X=0.05 , (c) X=0.10, (d) X=0.15

(e) X=0.20 , (f) X=0.25

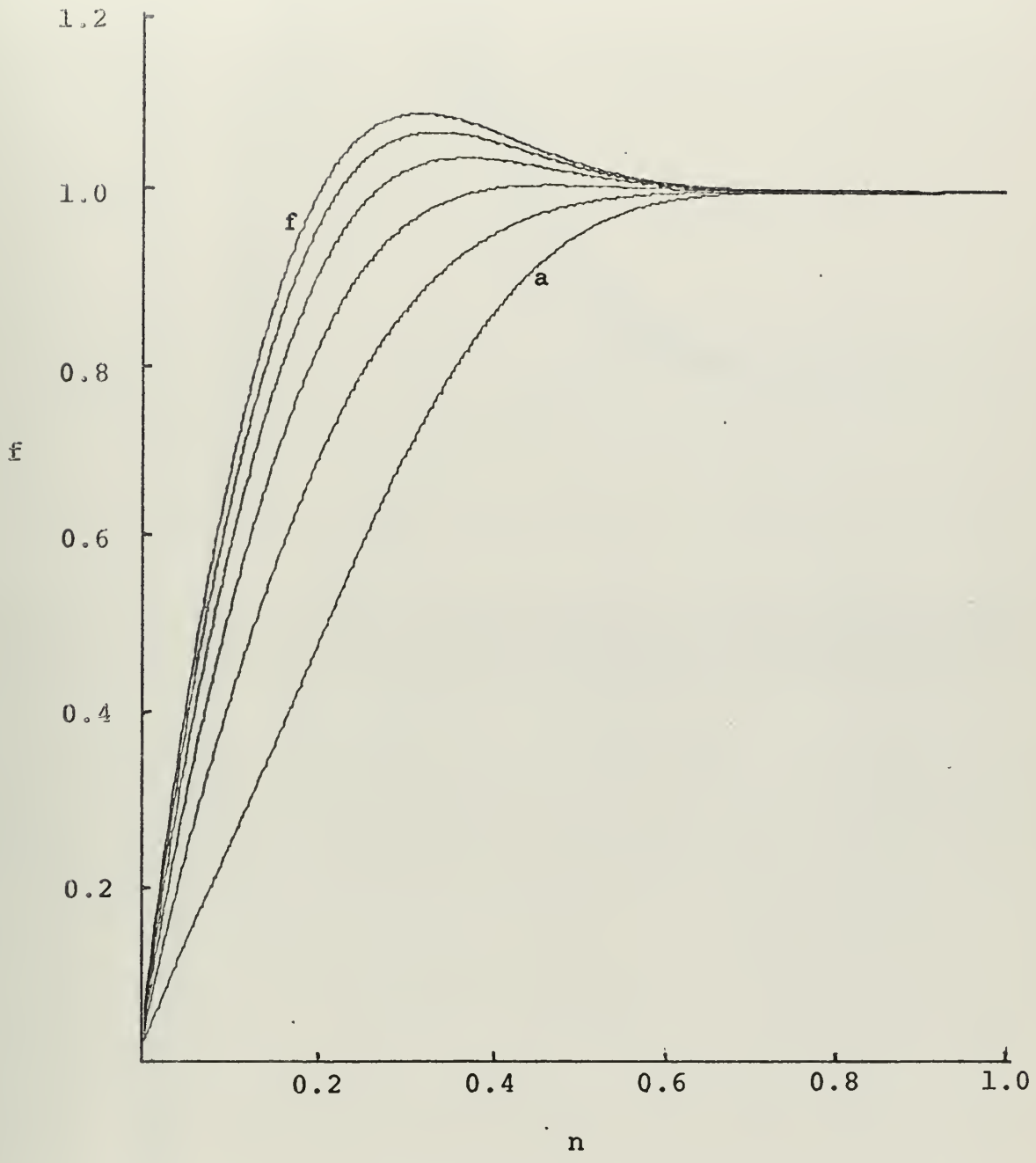

FIGURE 5. VARIATIONS IN PROFILE WITH X. K=2 G(0)=0.52

(a) X=0.00 , (b) X=0.05 , (c) X=0.10 , (d) X=0.15

(e) X=0.20 , (f) X=0.25

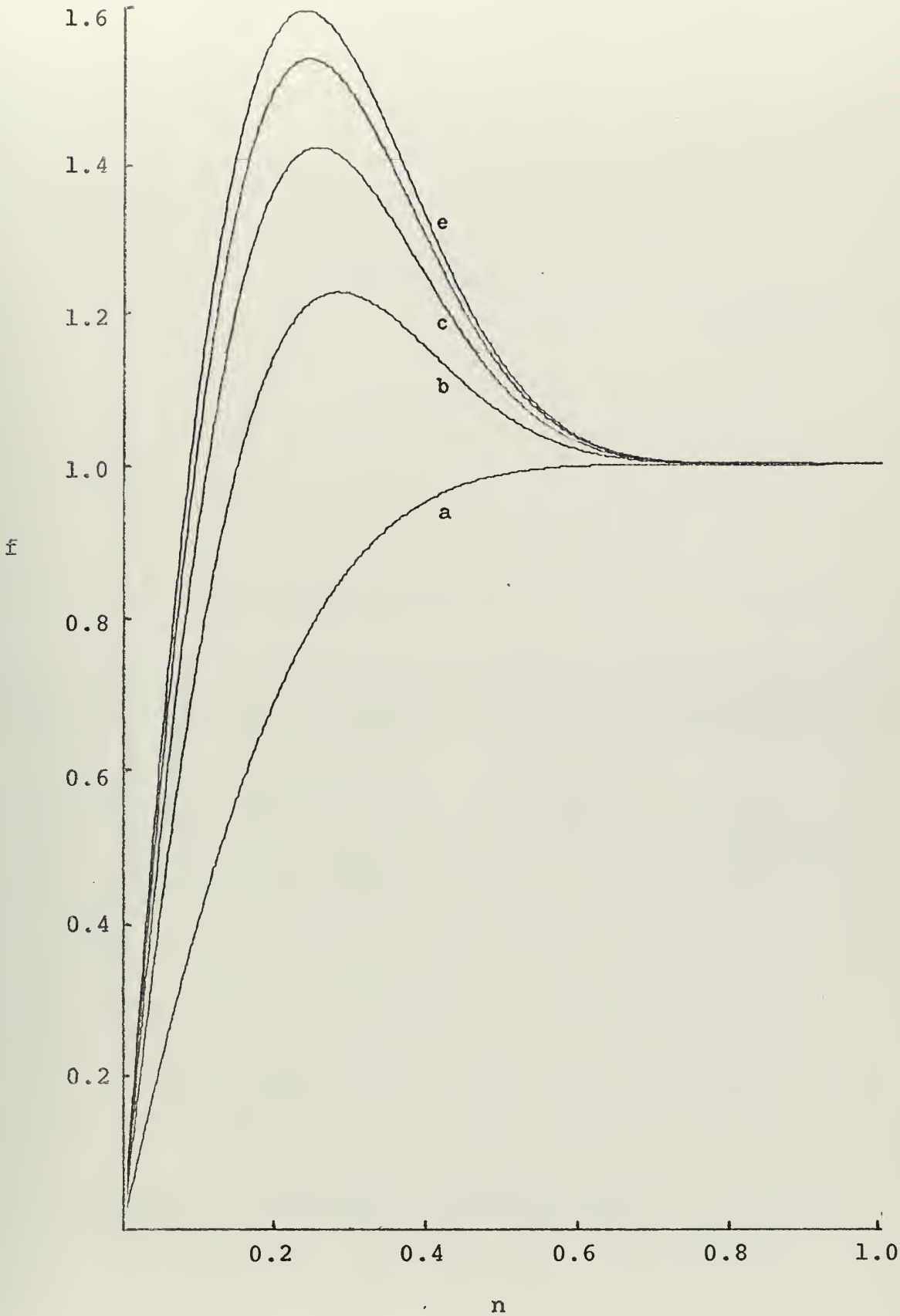

FIGURE 6. VARIATIONS IN PROFILE WITH X. K=4 G(0)=0.52

(a) X=.00 , (b) X=.05 , (c) X=.10 , (d) X=.15 , (e) X=.20

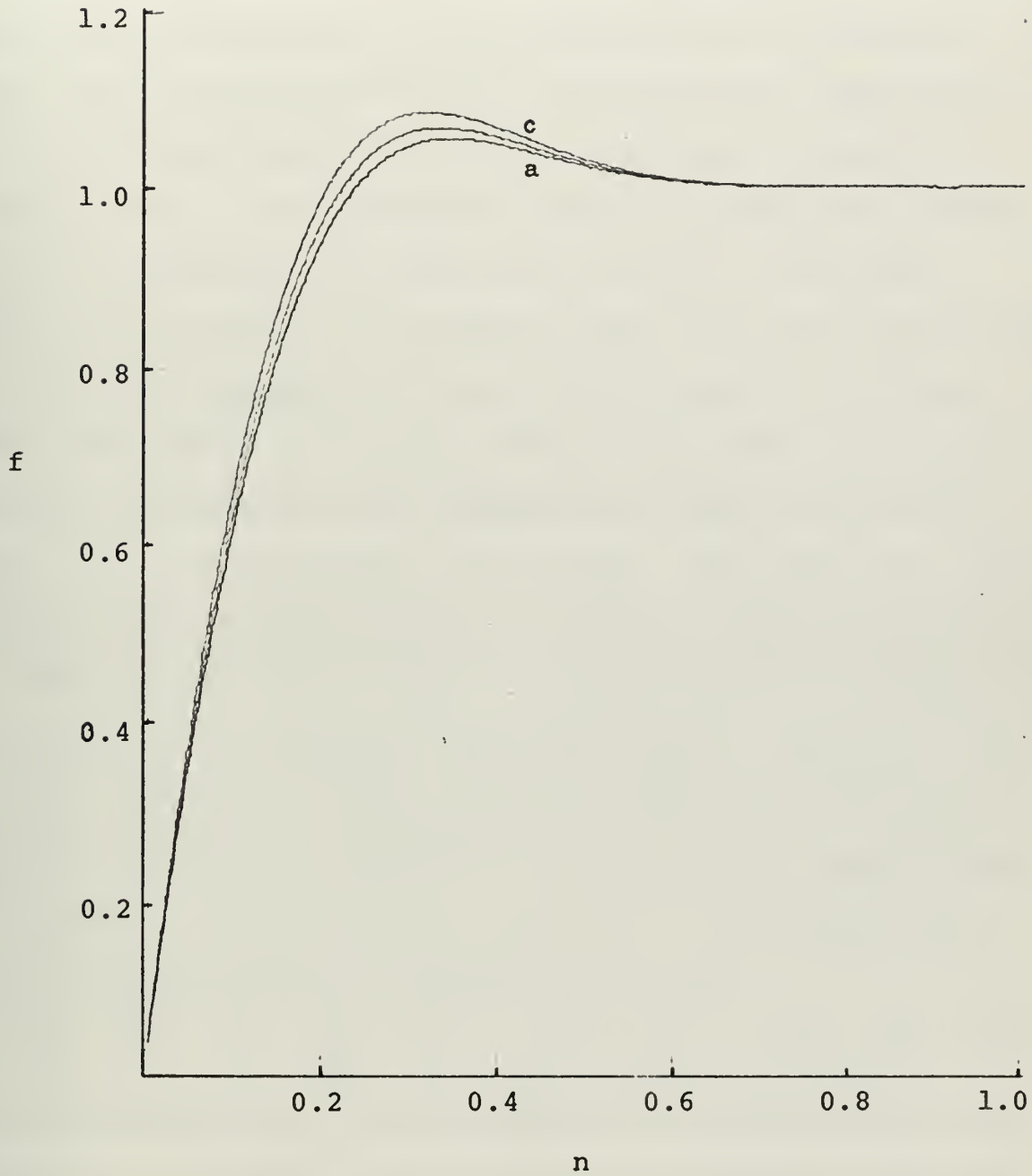

FIGURE 7. VARIATIONS IN PROFILE WITH G. K=2 X=0.2

(a) $\delta(0)=0.00$, (b) $\delta(0)=0.10$, (c) $\delta(0)=0.15$

C. PRESENT THEORY

The Wilks approach to the momentum equation assumed that the tangential velocity at the outer edge of the boundary layer could be described as A/r. This was only appropriate if the boundary-layer thickness was very small compared to the value of r. The numerical solution of the Wilks method led to a boundary-layer growth that could be of the same order as r for flow in air where r_o was about one inch and the initial axial velocity was one foot per second. In these cases, the radius minus the boundary-layer thickness should be used to determine the tangential velocity at the outer edge of the axial boundary layer rather than using the radius alone. Thus $V = A/(r - \delta)$.

The introduction of this new value of V into the boundary conditions of the momentum equations led to a different form of the v momentum-integral equation. The derivation of the equation is shown in APPENDIX B. This approach required the definition of a new thickness coefficient A5 (APPENDIX B). The v momentum-integral equation then became

$$\frac{r'}{r} + \frac{U'}{U} + \frac{\delta'}{\delta} + \left\{\frac{r'}{r} + \frac{V'}{V} + \frac{A5}{r/\delta - 1}\left(\frac{\delta'}{\delta} - \frac{r'}{r}\right)\right\} = \frac{A4}{G} \qquad (15)$$

In the above equation, Wilks assumption of a basically linear relationship between the characteristic thicknesses was used. The terms in the braces are added to the Wilks v momentum-integral equation by the new assumption, vix., $V = A/(r - \delta)$.

If the boundary layer is thick enough to effect the boundary condition for the tangential flow, the calculation

of the axial velocity should also take this boundary-layer growth into consideration. In using the conditions of continuity of flow, the radius minus the displacement thickness should be used rather than the radius alone. The displacement thickness, by its definition, is the distance the potential flow has been displaced by the presence of the boundary layer. The effect of this consideration would be to increase the axial core velocity as the displacement thickness grew.

D. NUMERICAL SOLUTION OF PRESENT THEORY

In order to calculate U and its derivative, U', the value of the displacement thickness and its derivative were needed. The ratio of the displacement thickness to the boundary-layer thickness was one of the integrals used in the calculation of the thickness coefficients. The boundary-layer thickness at any point could easily be calculated from the value of G once the kinematic viscosity and length of the nozzle to its apex had been specified. The calculation of the derivative of the displacement thickness was not as direct. Wilks based his solution on the assumption that a basically linear relationship existed between the momentum thickness and the boundary-layer thickness. An extension of this assumption would be to presume a basically linear relationship also existed between the displacement thickness and the boundary-layer thickness. Thus the ratio of the displacement thickness to its derivative should be equal to the ratio of the boundary-layer thickness to its derivative.

With the new equation for the v momentum integral, the numerical solution proceeded in the following manner:

(1) Using the initial boundary-layer thickness, the values of $G(0)$ and $L_2(0)$ were calculated.

(2) A predicted value for $L_1(0)$ was assumed from the Wilks solution for zero initial boundary layer thickness.

(3) The distance along a flat plate that would be required to produce a boundary-layer thickness of the same size as the initial boundary-layer thickness was calculated. Using this distance, the derivative of the boundary-layer thickness on a flat plate at this point was calculated. From this estimate of the derivative and assuming an initial value for Dl from the Wilks solution, the initial value of the derivative of U was evaluated.

(4) Using the current values of L_1 and L_2, the values of the thickness coefficients were calculated.

(5) The value of δ'/δ was calculated, where

$$\frac{\delta'}{\delta} = \left(\frac{A4}{G} - \frac{U'}{U} - \frac{r'}{r}\left(2 - \frac{A5}{r/\delta - 1}\right) - \frac{V'}{V}\right) \Big/ \left(1 + \frac{A5}{r/\delta - 1}\right) \qquad (16)$$

(6) The new value of L_1 was calculated from

$$L_1 = D2 \cdot G \cdot \left[\frac{U'}{U} (2 + A1) + \frac{r'}{r} \left(1 - \frac{V^2}{U^2} A3\right) + \frac{\delta'}{\delta} \right] \tag{17}$$

(7) The calculated value of $L_1(0)$ was compared with the assumed value. If the two values were not sufficiently close, the thickness coefficients and velocities were re-evaluated until the values of $L_1(0)$ for two consecutive iterations were sufficiently close.

(8) The value of G' was determined from

$$G' = G \left(2\frac{\delta'}{\delta} + \frac{U'}{U}\right)$$

(9) The values of G and L_2 for the next point were then calculated.

(10) The step-by-step evaluation of the momentum-integral equations was continued for new values of X by returning to step 4 and remembering that step 7 is used only when X=0.

U and V as functions of X are given in APPENDIX B.

Using this numerical technique, the momentum-integral equations were solved for various values of initial boundary-layer thicknesses, initial velocities, and K. Since this method required the division by G in the calculation of equation 16, the analysis was not valid for the case where the initial boundary-layer thickness was zero. However, for very

small values of G other than zero, there was no restriction on the initial boundary-layer thickness. The solution of these equations showed no sign of super-velocity. In several cases the step-by-step evaluation continued smoothly for values of X up to 0.6. The boundary-layer growth reached a maximum value when X was in the range of 0.25 and then decreased with X. This numerical analysis appeared to lose its validity when the momentum thickness became negative, which occurred at a much higher value of X then in the Wilks solution. At this value of X where the momentum thickness became negative, discontinuities appeared in the boundary-layer growth. Figures 8-12 show a comparison between the profiles of the Wilks solution, as modified for initial boundary-layer thickness, and the profiles obtained by the above method.

E. DISCUSSION OF THEORETICAL RESULTS

Wilks based his solution of the flow in the boundary layer of a convergent nozzle on several assumptions. He first considered the inviscid core as a free vortex with uniform axial flox. It was then assumed that the boundary layer would be thin enough to prevent any effect of its growth upon the core velocities. Thus the core velocities were dependent only upon the geometric configuration of the convergent nozzle. Wilks also assumed that a linear relationship existed between the various characteristic thicknesses of the boundary layer. With these assumptions, the solution of the momentum-integral equations led to the existence of a super-velocity in the boundary layer.

For low velocity air flow (required to maintain the laminar conditions) the boundary-layer growth was not negligible. By including this growth in the calculations of the boundary conditions, the solution no longer led to super-velocities. Increased swirl only decreased the ratio of the displacement thickness to the boundary-layer thickness slightly.

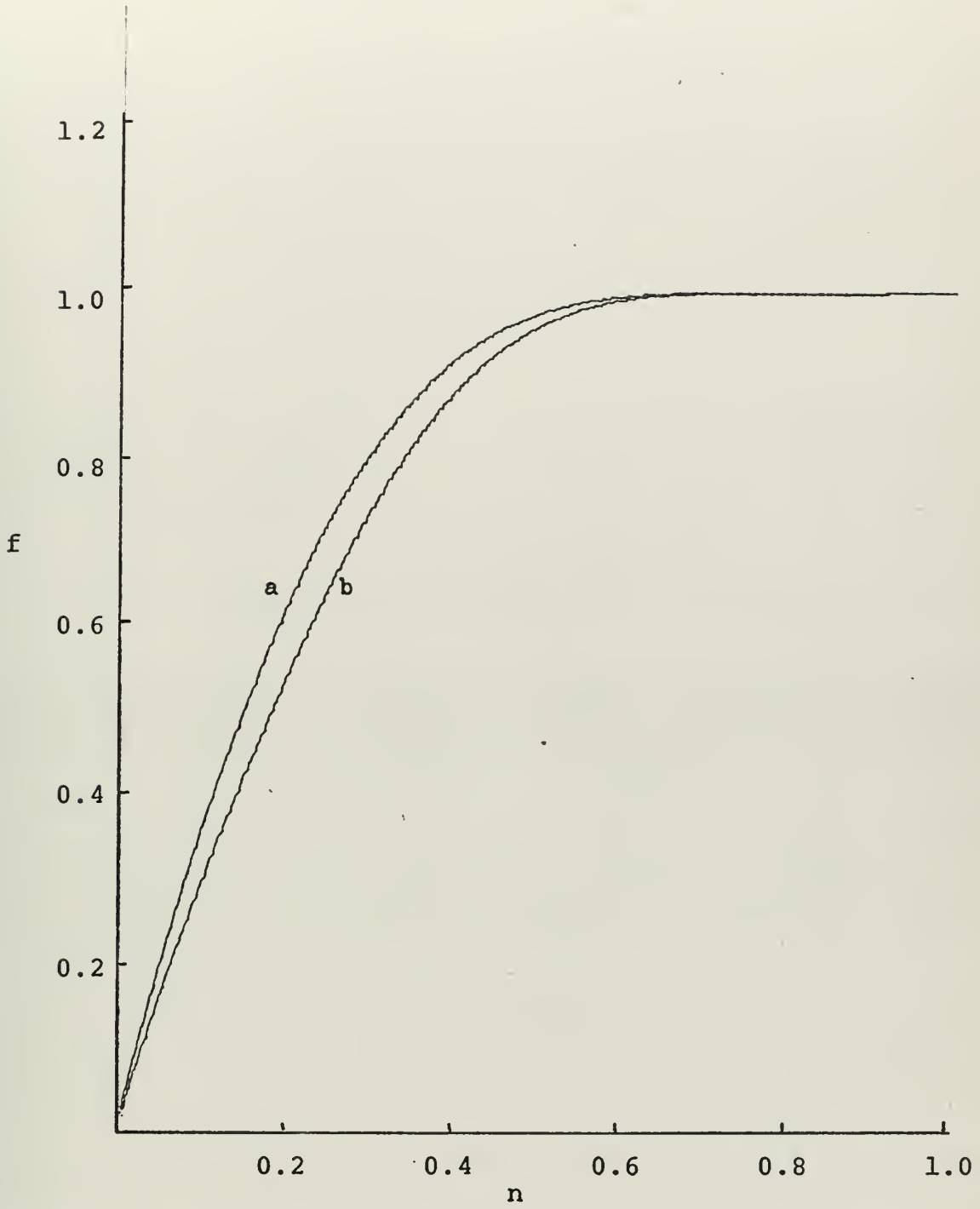

FIGURE 8. COMPARISON OF THEORETICAL CURVES. K=1 x=.1 $G(0)=0.52$ $\delta(0)/r_o=0.130$ (a) Wilks theory , (b) present theory

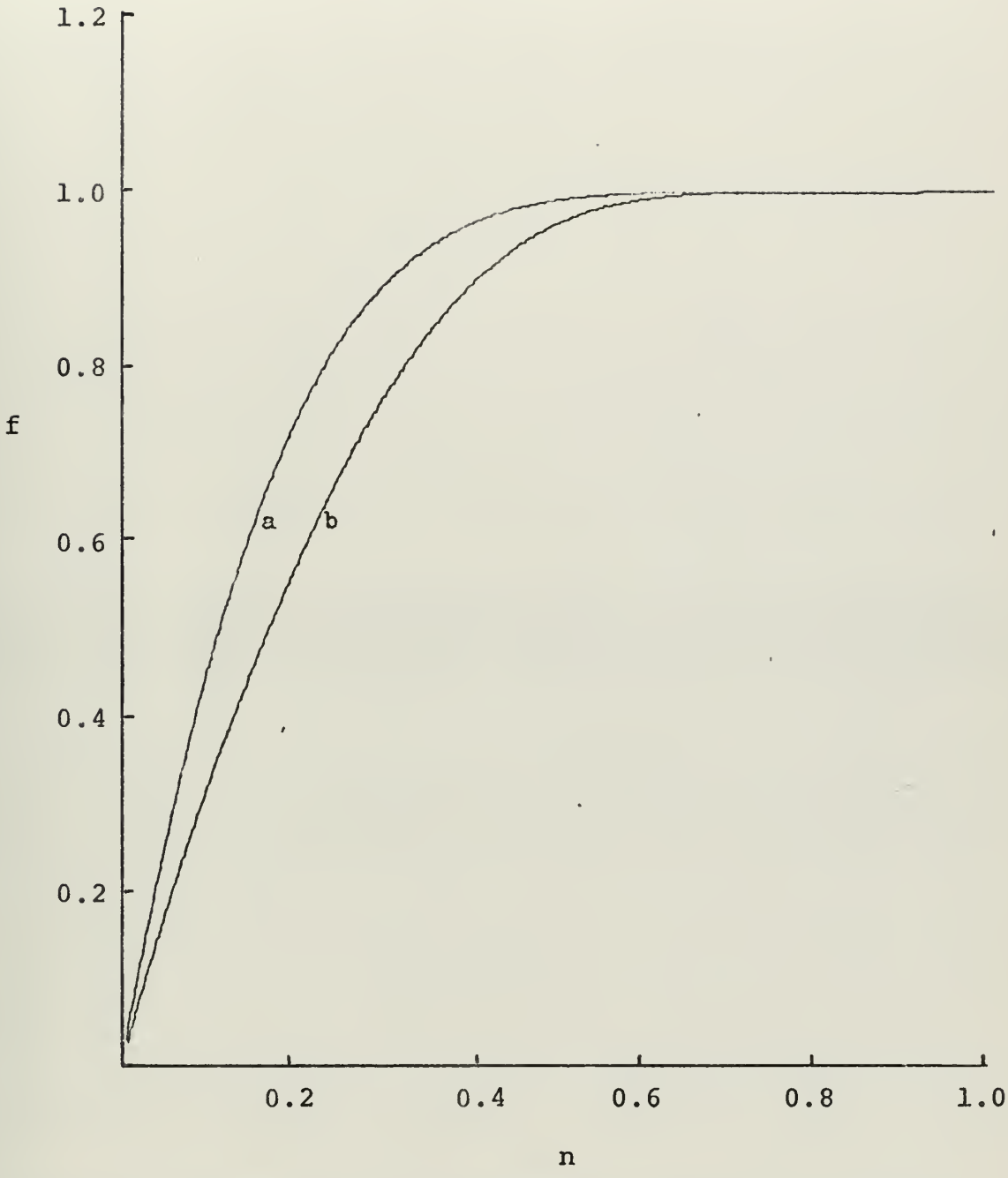

FIGURE 9. COMPARISON OF THEORETICAL CURVES. K=1 X=0.2 G=0.52 $\delta(0)/r_o$=0.130 (a) Wilks theory , (b) present theory

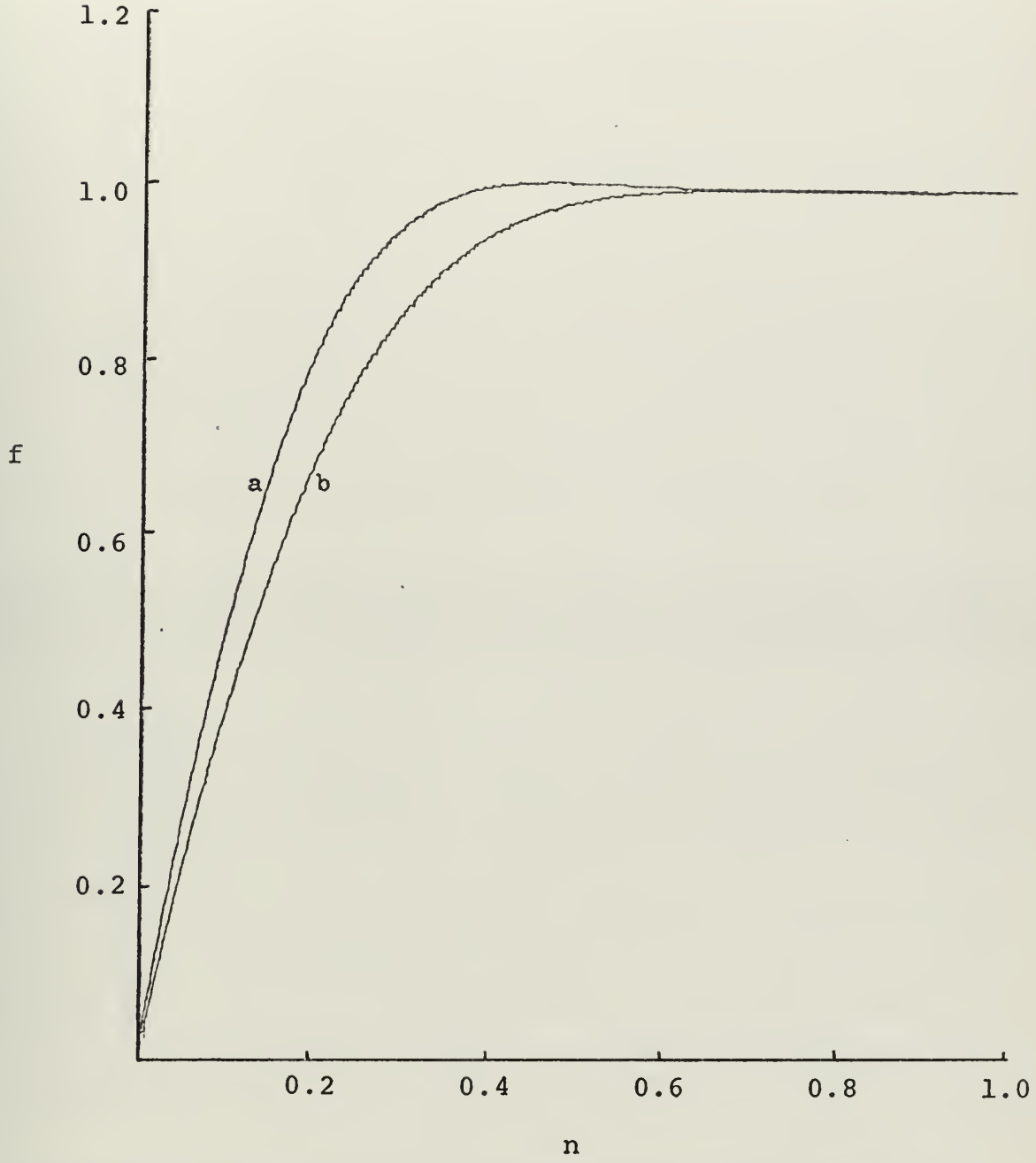

FIGURE 10. COMPARISON OF THEORETICAL CURVES. K=2 X=0.1 G(0)=0.52 $\delta(0)/r_o$=0.130 (a) Wilks theory , (b) present theory

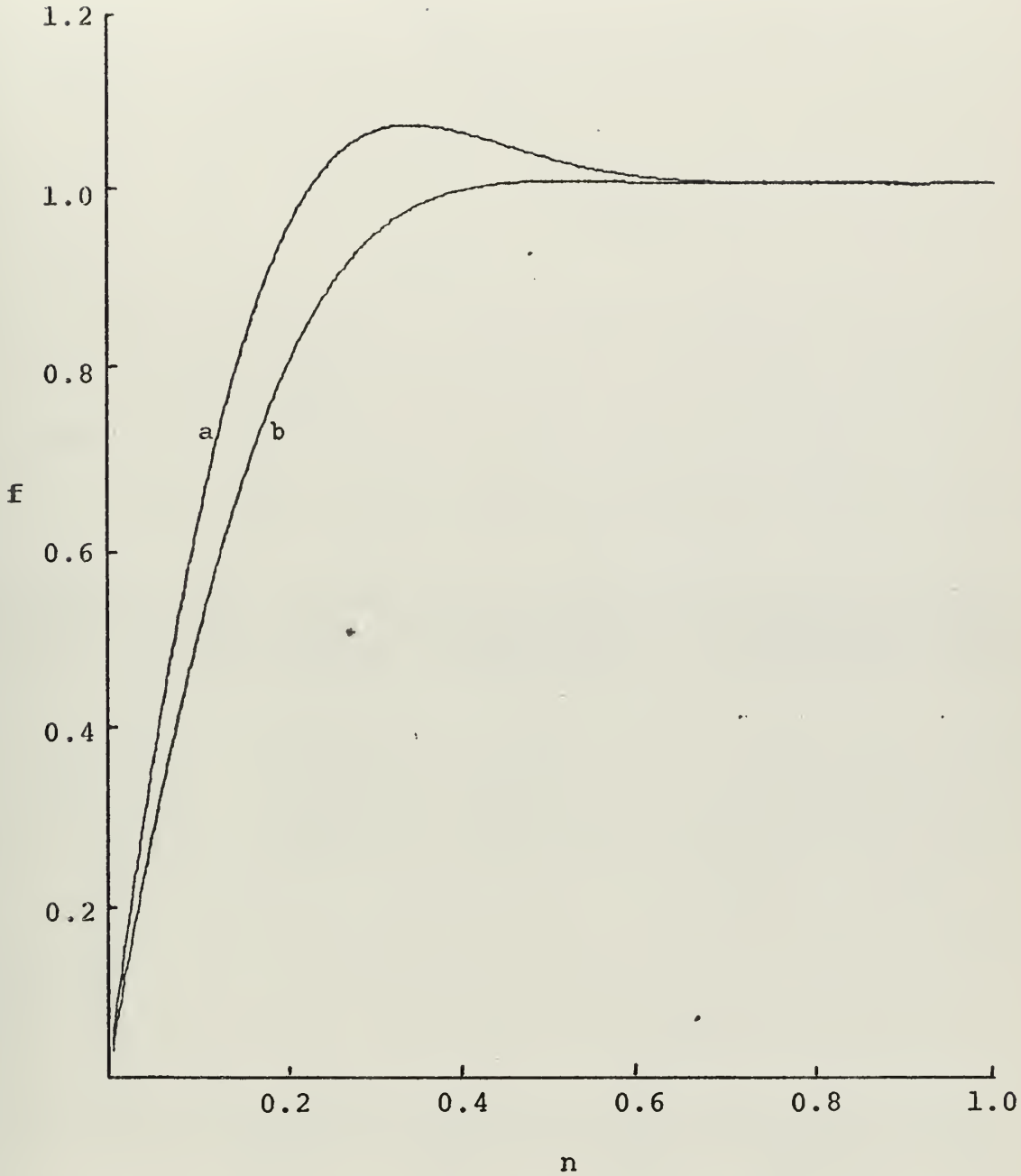

FIGURE 11. COMPARISON OF THEORETICAL CURVES. K=2 X=0.2 G(0)=0.52 $\delta(0)/r_o$=0.130 (a) Wilks theory , (b) present theory

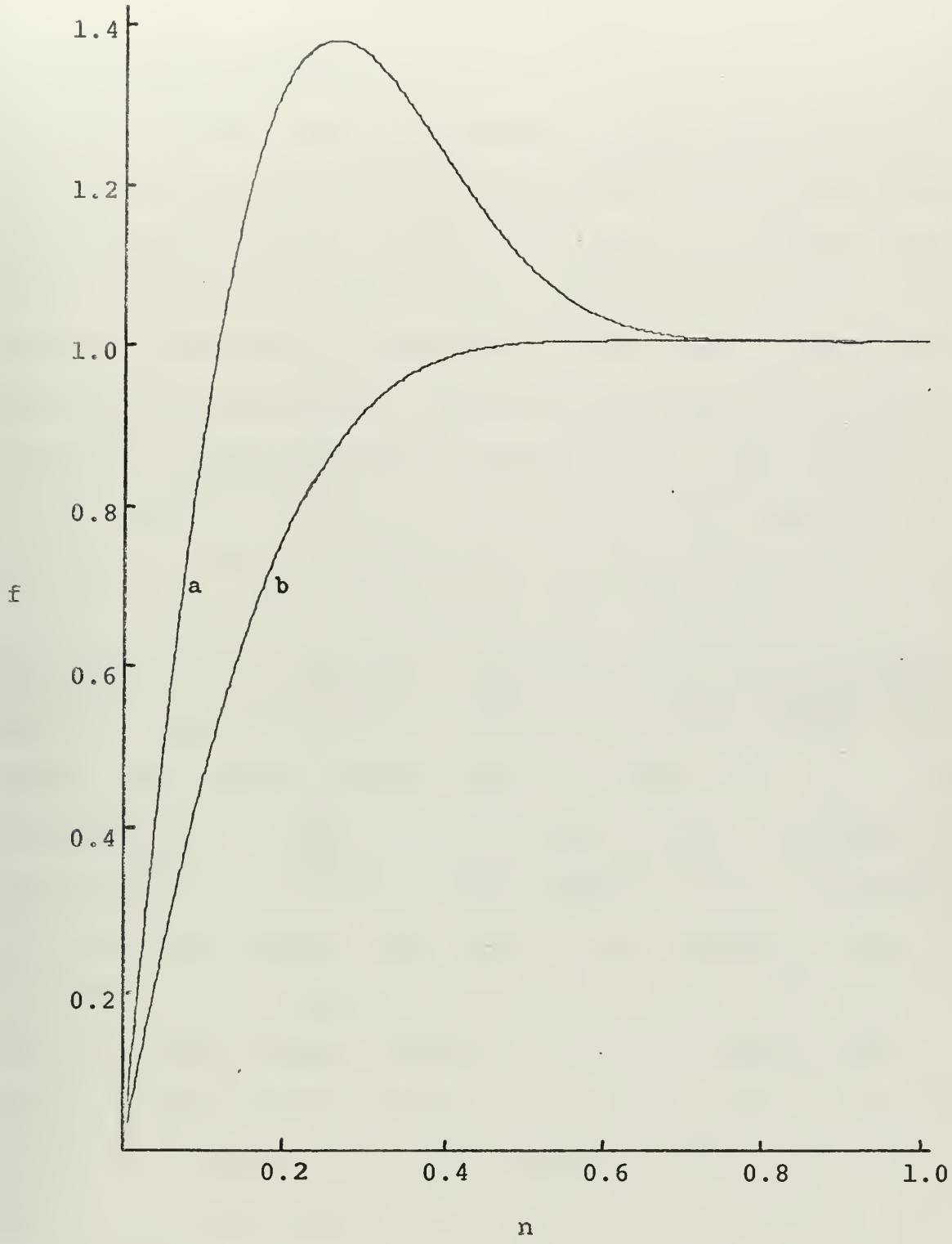

FIGURE 12. COMPARISON OF THEORETICAL CURVES. K=4 X=0.1 G(0)=0.26 $\delta(0)/r_o$=0.065 (a) Wilks theory , (b) present theory

III. EXPERIMENTATION

A. DESIGN OF APPARATUS

The analytical approach assumed that the flow entering the convergent nozzle was a combination of a free line-vortex and uniform axial flow. To test the theory, an apparatus was required to approach this assumed velocity distribution. There are several methods of introducing a fluid into a chamber and causing a swirling motion. However, this tangential velocity would have to approximate the conditions of a free vortex, that is the tangential velocity should be inversely proportional to the radius. Several methods were considered, including rotating a section of the swirl-producing chamber, drawing the fluid into the chamber from a stagnation condition while using vanes to create the tangential motion, and rotating blades inside the chamber. The approach chosen was to introduce the fluid through one tangential port with variable cross-section. In tests of a Hilsch tube, Lay [4] used a single circular port to introduce a jet into the chamber. This was the only source of fluid in his tests, and he reported the velocity profiles that were produced in this manner. However, he did not indicate the radial profile of the velocities in a region close to the wall. The results indicated that the tangential flow might closely approximate the conditions for a free vortex over most of the radius, departing from these conditions in the center portion. The distribution of the axial velocity in Lay's tests suggested that the superposition of pipe flow upon this flow could result in a nearly uniform axial flow.

The source of fluid for this apparatus was a compressed air tank. To insure laminar pipe flow of the air at speeds of at least two feet per second, a pipe diameter of two inches was chosen. Axial pipe-flow could be produced prior to entry of the axial flow into the swirl chamber. The shape of this axial flow could be varied by adjusting the axial position of a honeycomb flow-straightener. If profiles different from pipe flow were required to achieve the uniform axial profile at the entrance of the cone, the flow could be adjusted by only passing air through selected annular portions of the honeycomb flow-straightener.

The tangential flow was introduced through a rectangular slot in the wall of the swirl generator. One wall of this slot was tangent to the inner surface of the chamber. The slot was 0.25 inches high and the width could be varied from 0.3 to 1.25 inches. This variable cross-section permitted an adjustment in the ratio of the velocity to the quantity of mass introduced by the tangential port. This flexibility in the system was added to insure that the proper profiles and values of K could be obtained. Tests were then performed to determine the axial distance required for the development of the appropriate flow conditions. These preliminary tests indicated that a range between one and two feet was required for the development of the tangential jet into a free vortex.

Lay's tests indicated that there would be a region close to the wall where the tangential flow would be retarded by

viscosity. An axial combination of pipe flow and the tangentially introduced flow would also have a region close to the wall where the conditions for uniform axial flow would not be met due to the viscous forces present. With these two boundary-layer growths under consideration, the outer annular portion of the flow was bled off, with only the "flat" inner portion of the axial flow entering the cone. This bleed-off was accomplished by placing a cone of initial radius 0.77 inches at the end of the tube which had an inside radius of one inch. The position of the cone relative to the end of the tube could be varied in order to alter the amount of flow bled off into the atmosphere. The entry region into the cone consisted of a one-inch straight section. The purpose of this section was to insure the continuation of the proper flow characteristics after bleed-off. (See Figure 25)

The cone, a piece of machined plexiglass, featured a semi-angle of 4.4 degrees. The distance along the generator of the cone to the apex, termed c in the analysis, was ten inches. The truncated cone used in the test apparatus extended over 0.35 c. Thus, tests could easily be performed over the region where X varied from 0.0 to 0.3. Two hot-wire probes were introduced from the exhaust end of the truncated cone. One configuration was sensitive to axial and radial components alone. The other probe could detect tangential and radial velocities. It was assumed that the radial component of flow was negligible, especially close to the wall. The traversing

mechanism moved in two directions, allowing for motions in both the x-direction and the z direction.

B. EXPERIMENTAL RESULTS

The development of flow conditions that would approximate the desired conditions was basically a trial-and-error procedure. By adjusting the slot width, the development length for the tangential flow (by changing the length of pipe between the swirl generator and the nozzle), the bleed-off level, and the radial distribution of the axially introduced flow, it was possible to achieve several flow conditions that approximated the analytical boundary conditions at the entrance of the cone. However, in all the cases tested, the velocity distribution in the inviscid core changed drastically with X. The radial distribution of the axial and tangential velocities for several values of X with swirl ratios (K) of 0.6, 0.8, and 0.95 are shown in Figures 13-24. These profiles indicate several different flow relationships. For the case where K=0.6, the degree of swirl had very little effect upon the axial flow as it moved through the cone. The uniform axial core was gradually replaced by a flow that resembled the distribution in pipe flow, with most of the flow occuring in the central portion, and the perimeter retarded by viscous forces. With the slight increase to K=0.8, there was a great change in the radial distribution of the axial flow. In this case, the free vortex seemed to be maintained for all test stations. At X=0.3, this tangential motion had thrown a great deal of the fluid into the peripheral

portion of the cone, leading to a high axial velocity near the wall. However, this high velocity was still in the core (z=0.2 inches) and not in the boundary layer. In the tests where K=0.95, the distance over which the tangential flow appeared as a free vortex was less then in the previous cases. This smaller distance resulted in several changes in the tangential velocity with X. As a result of this changing tangential profile, there were several in the axial flow. In sections where the tangential flow appeared as a forced vortex, there was one form of axial flow, where high speed occurred away from the wall, while in annular sections where the tangential flow resembled a free vortex, the high speed axial flow occurred nearer the wall.

C. DISCUSSION OF EXPERIMENTAL RESULTS

In both of the analytical approaches, the inviscid core was considered a combination of uniform axial flow and a free vortex. In the test cases, the axial flow at the entrance of the nozzle was within five per cent of uniform axial flow. The tangential flow approximated a free vortex over most of the radius in the entrance region. However, this flow could not be maintained down the cone. Swirl induced a high velocity axial flow near the wall when the tangential flow was in the form of a free vortex. This region of high axial-velocity flow was far enough away from the wall (a distance greater than 0.15 inches) to call it part of the inviscid core. Thus swirl does

indeed cause changes in the axial flow, but these changes occur in the core and not in the boundary layer as Wilks suggested.

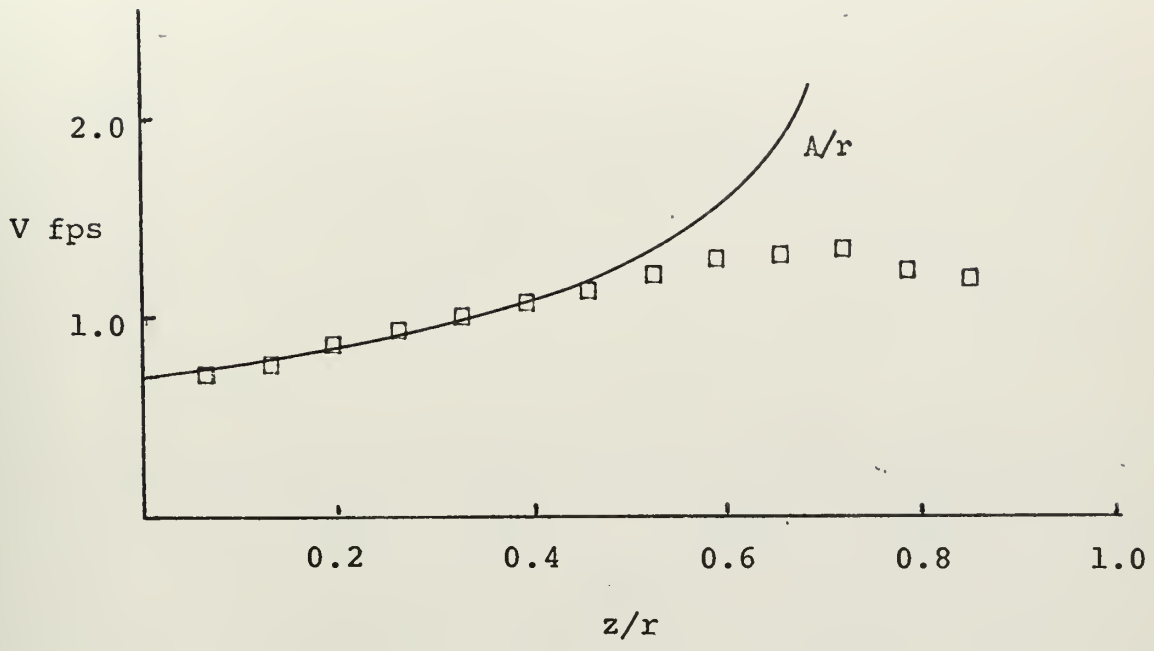

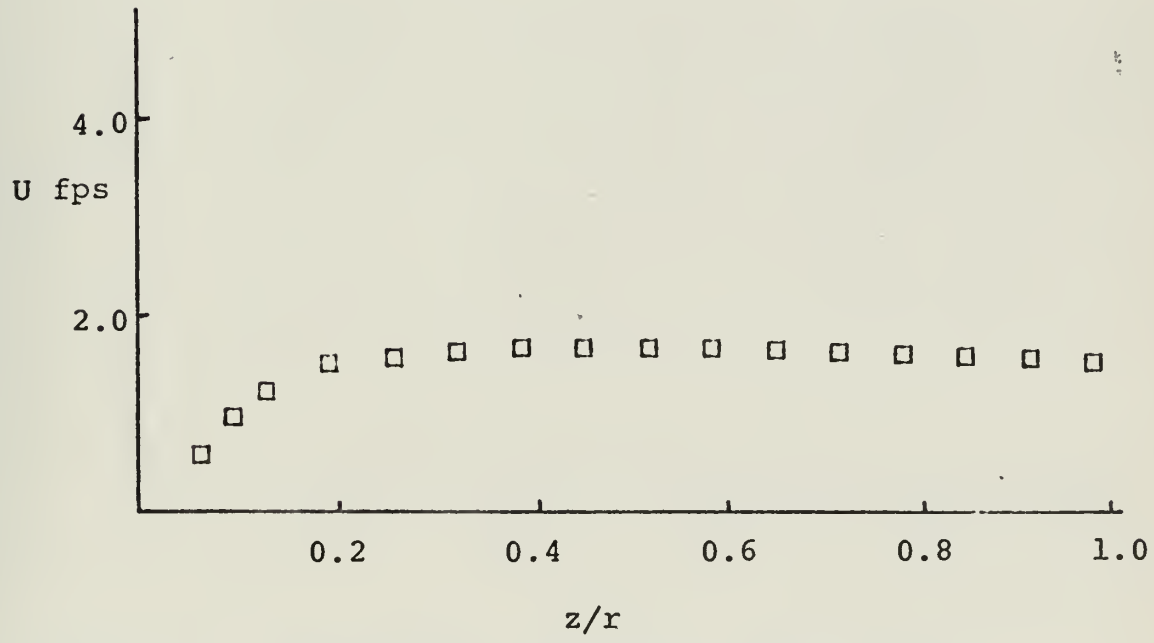

FIGURE 13. EXPERIMENTAL PROFILES K=0.6 X=0.0

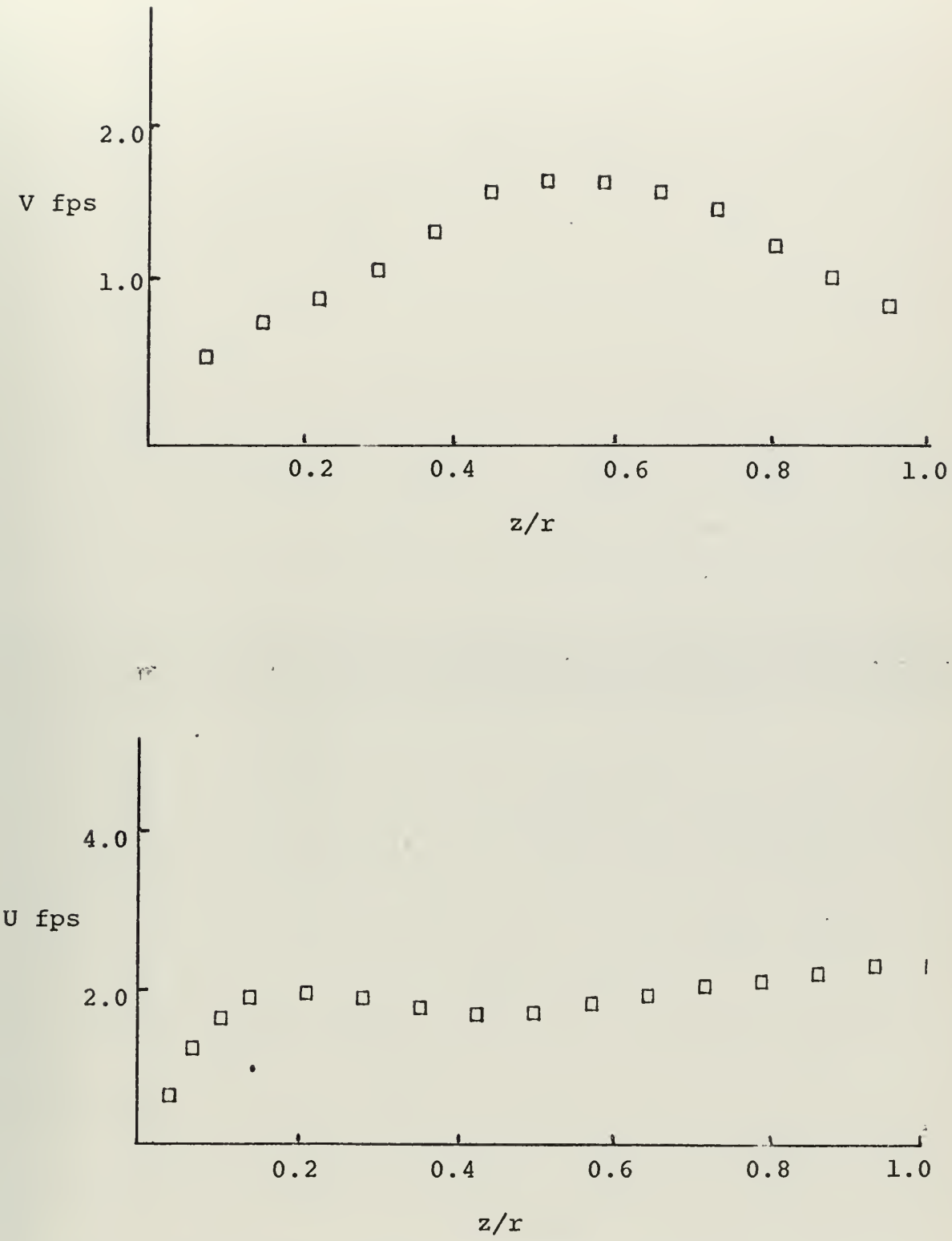

FIGURE 14. EXPERIMENTAL PROFILES. K=0.6 X=0.1

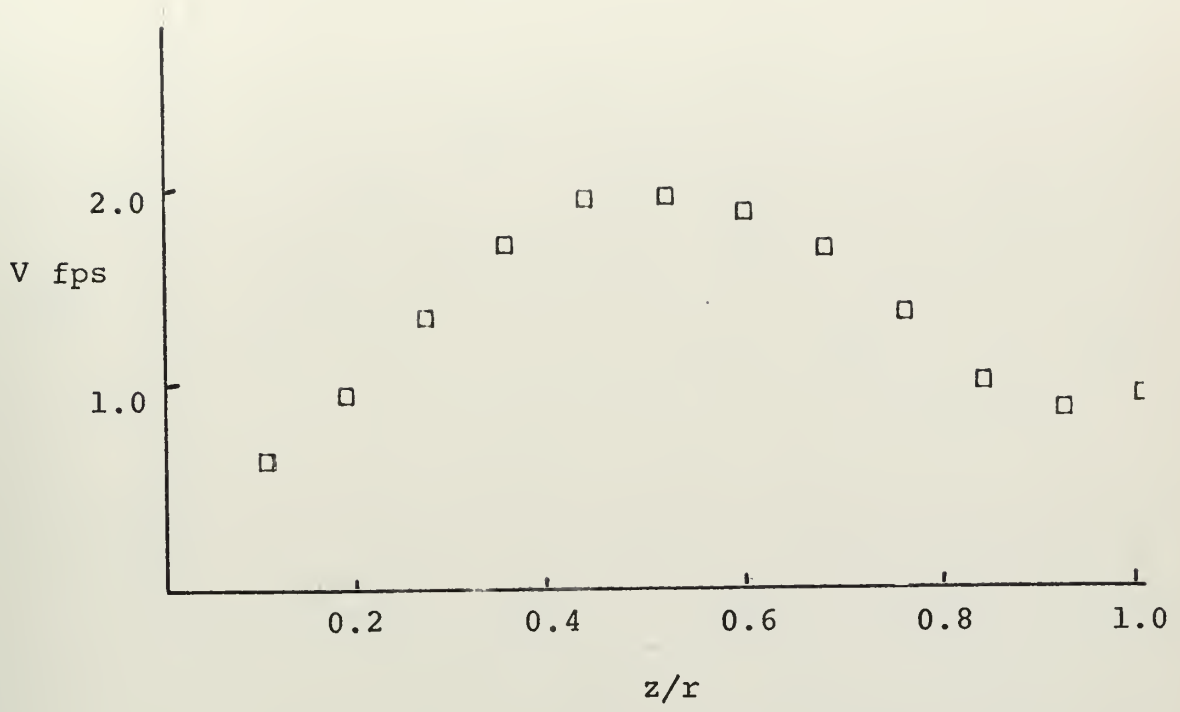

FIGURE 15. EXPERIMENTAL RESULTS. K=0.6 X=0.2

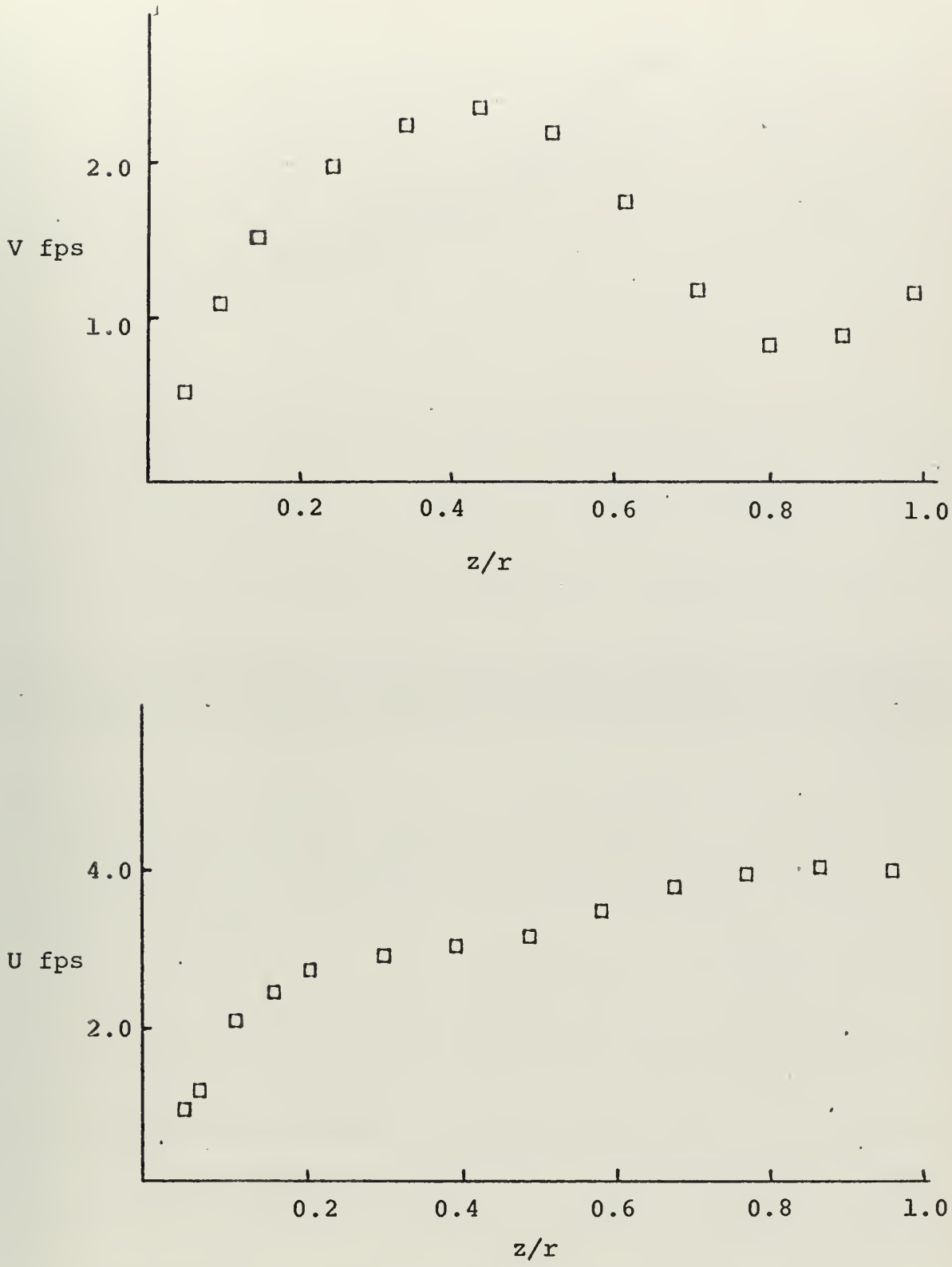

FIGURE 16. EXPERIMENTAL PROFILES. K=0.6 X=0.3

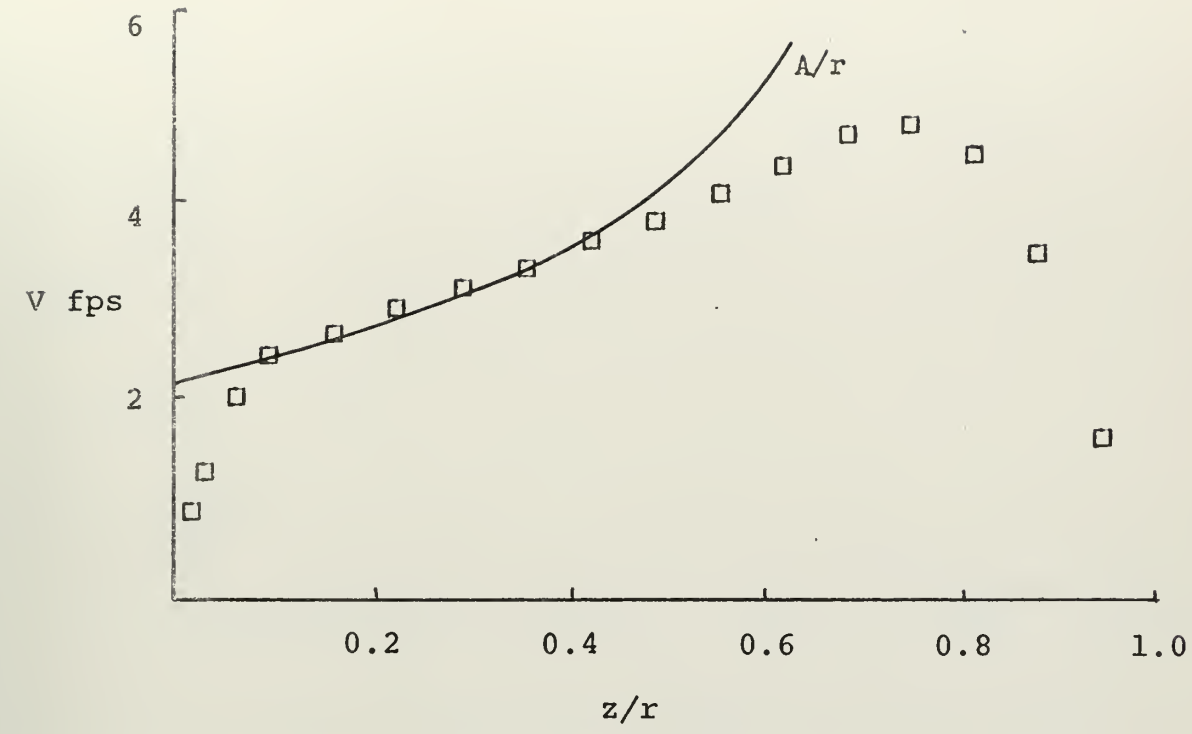

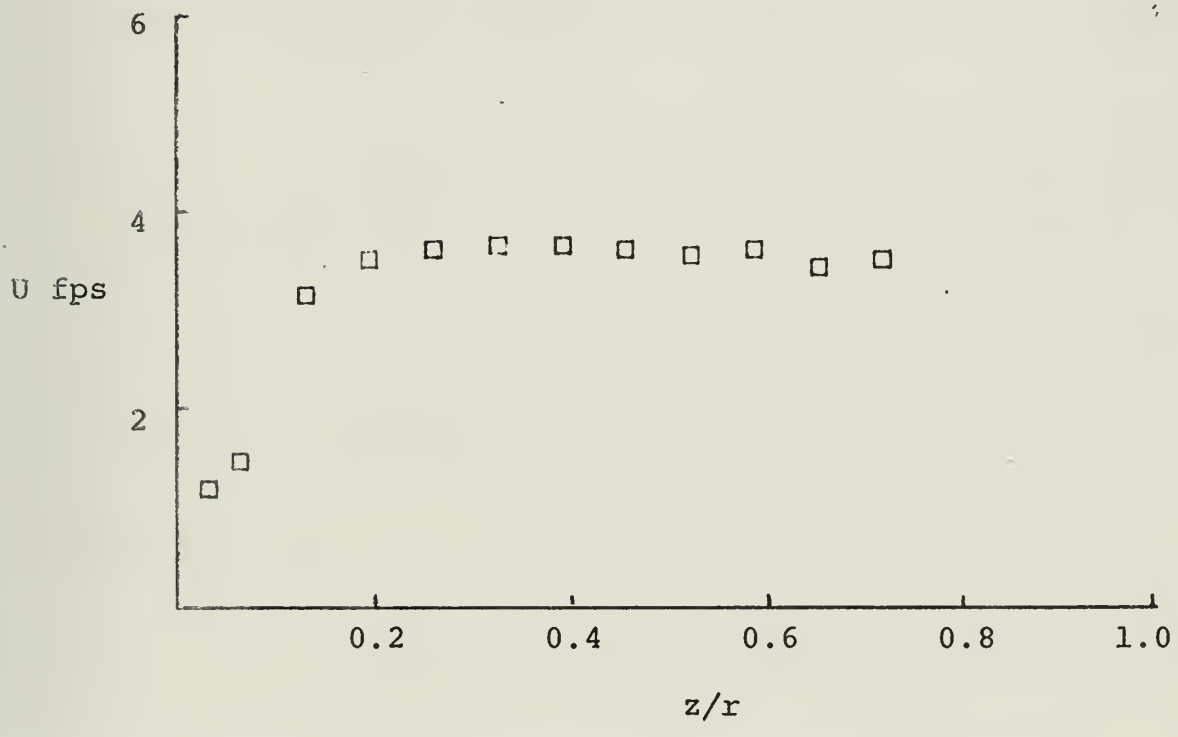

FIGURE 17. EXPERIMENTAL PROFILES. K=0.8 X=0.0

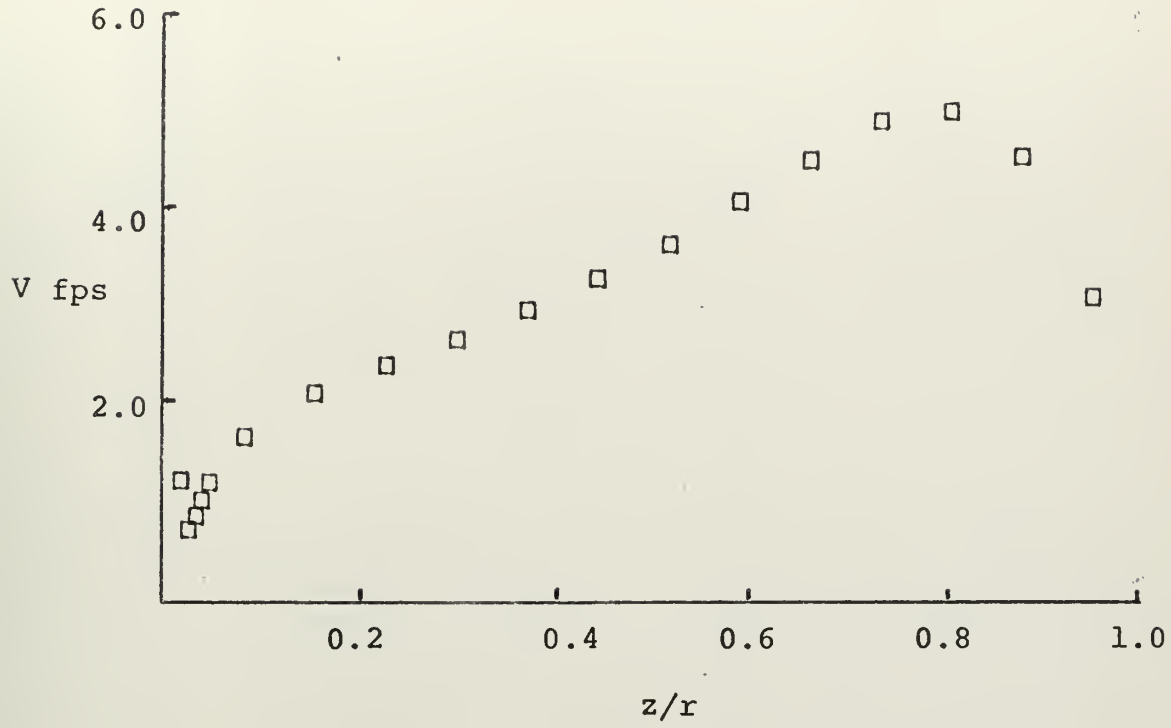

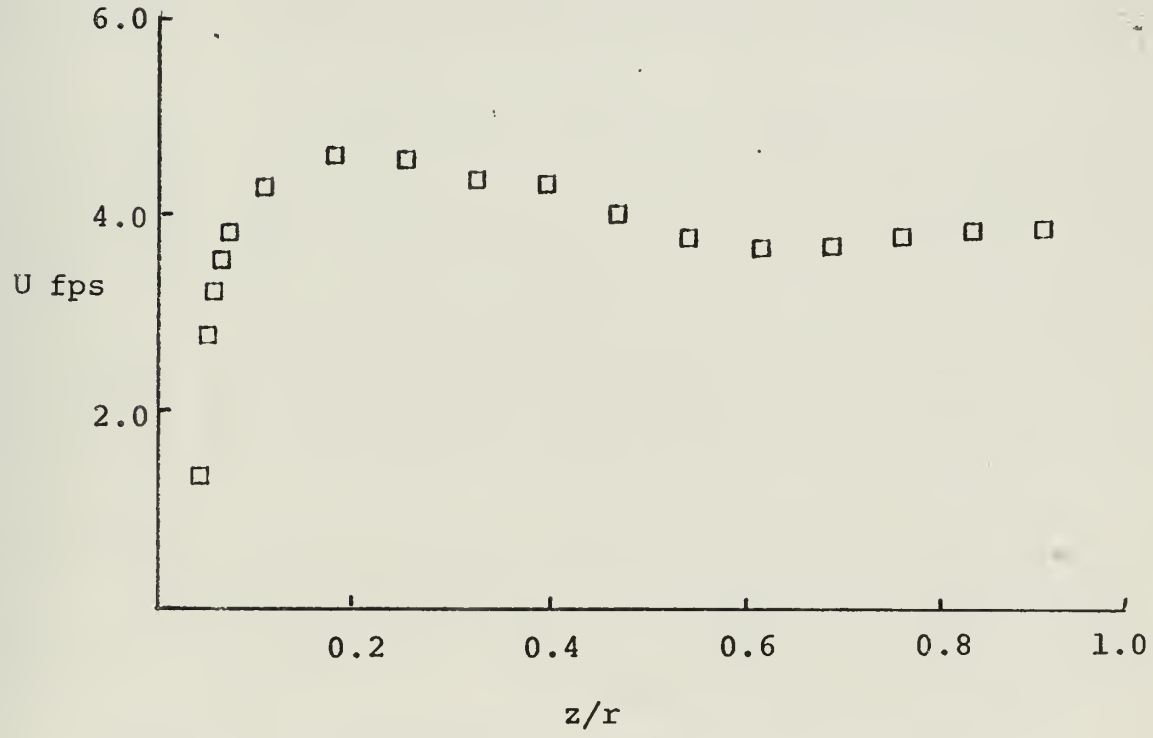

FIGURE 18. EXPERIMENTAL PROFILES. K=0.8 X=0.1

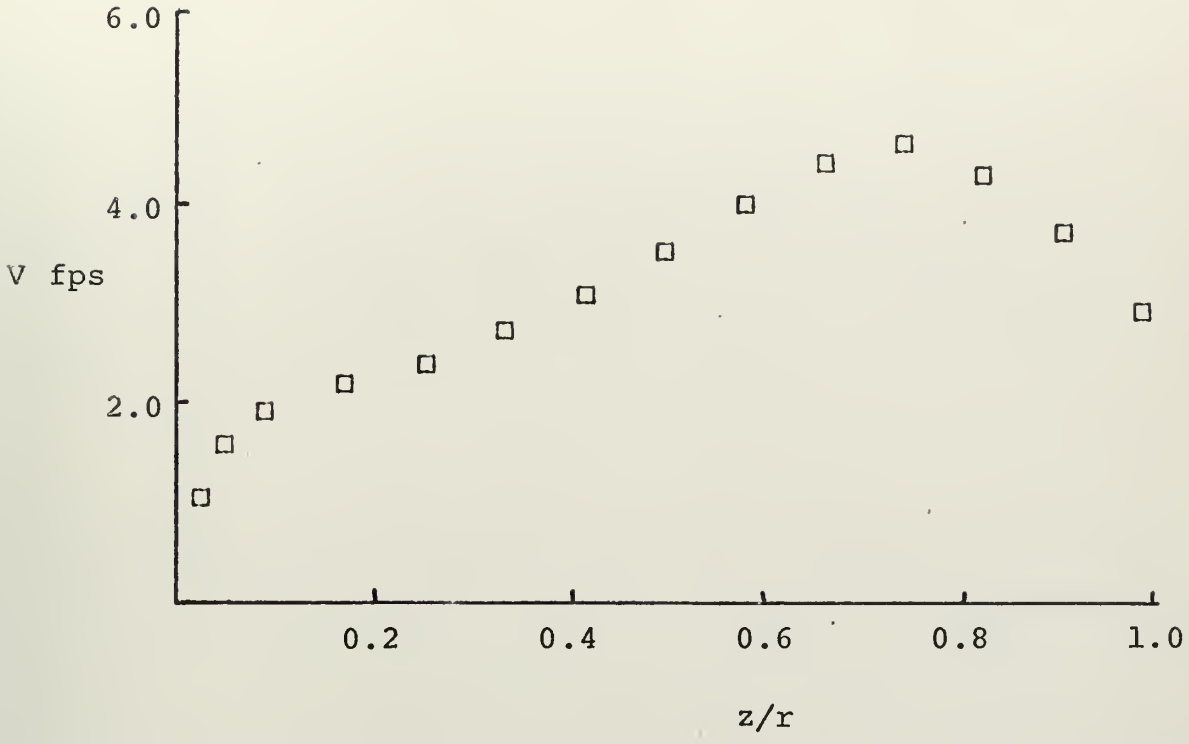

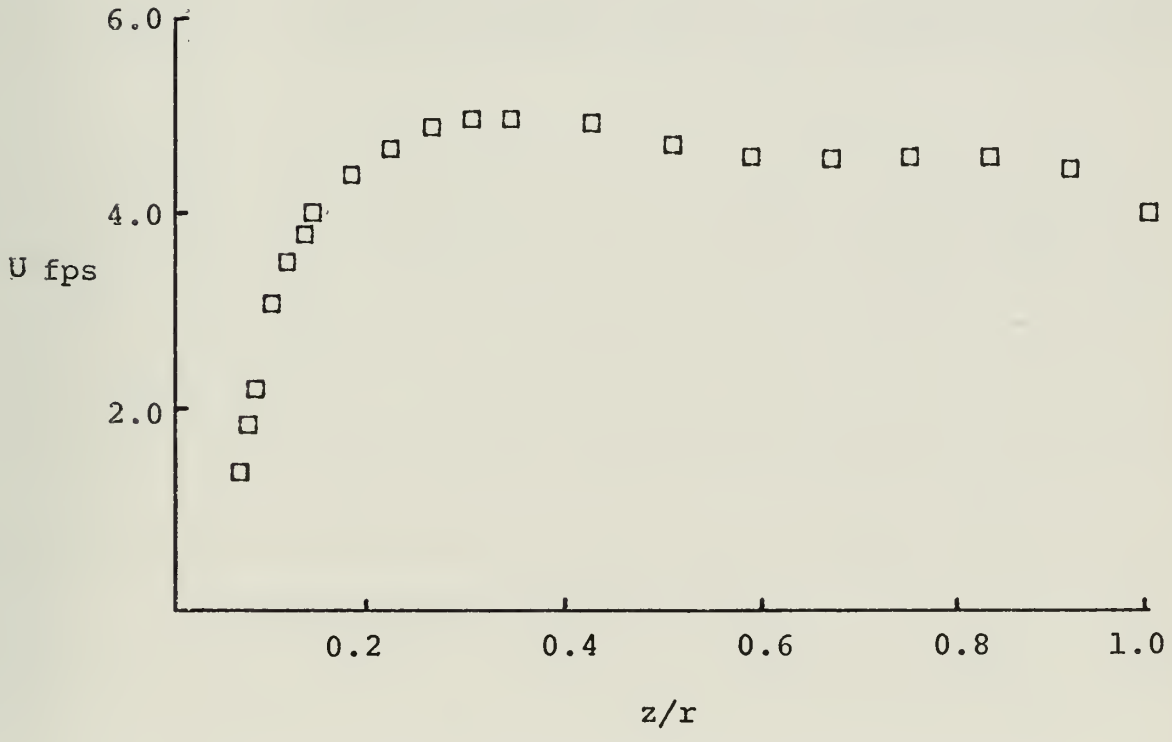

FIGURE 19. EXPERIMENTAL PROFILES K=0.8 X=0.2

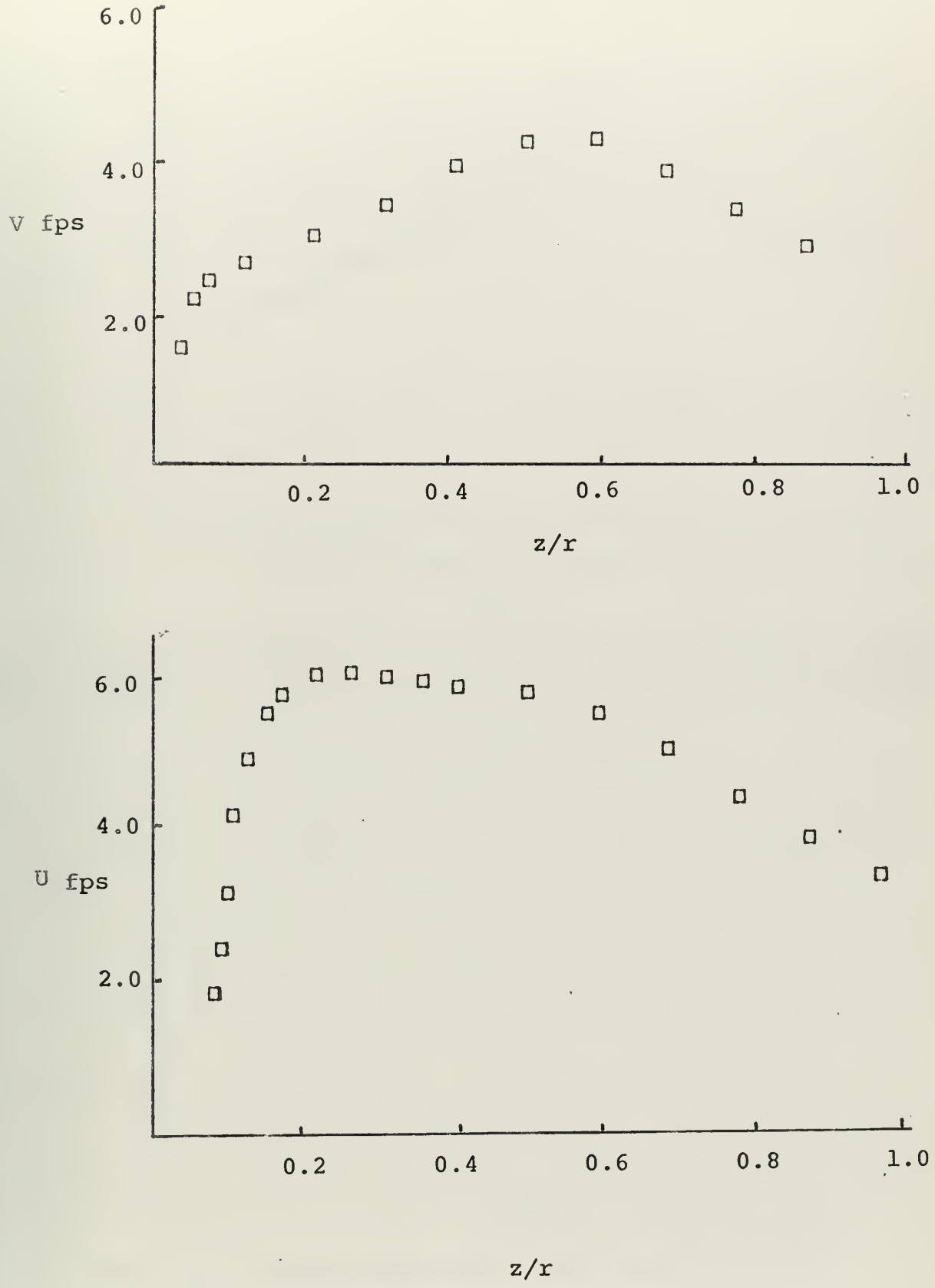

FIGURE 20. EXPERIMENTAL PROFILES. K=0.8 X=0.3

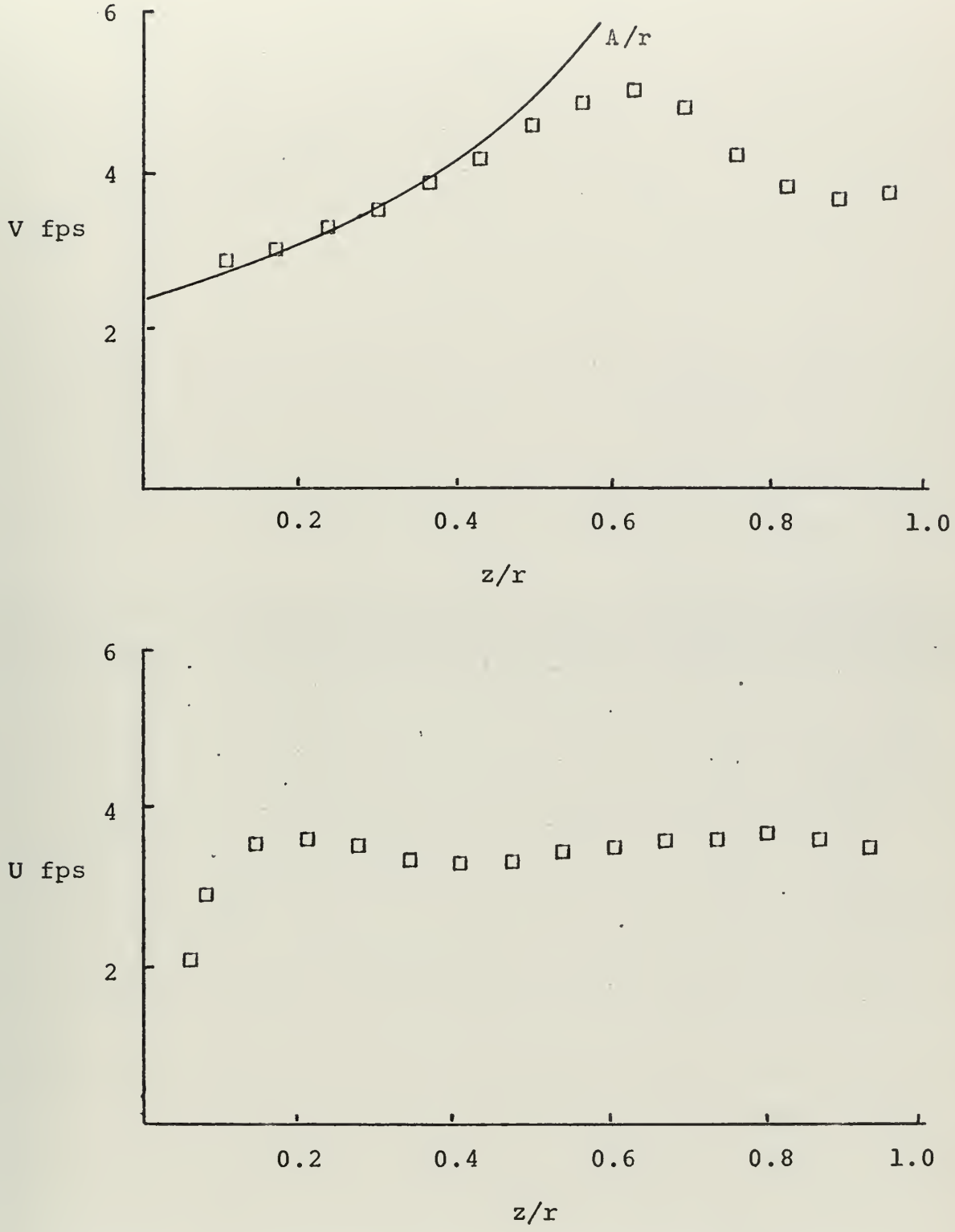

FIGURE 21. EXPERIMENTAL PROFILES. K=0.95 X=0.0

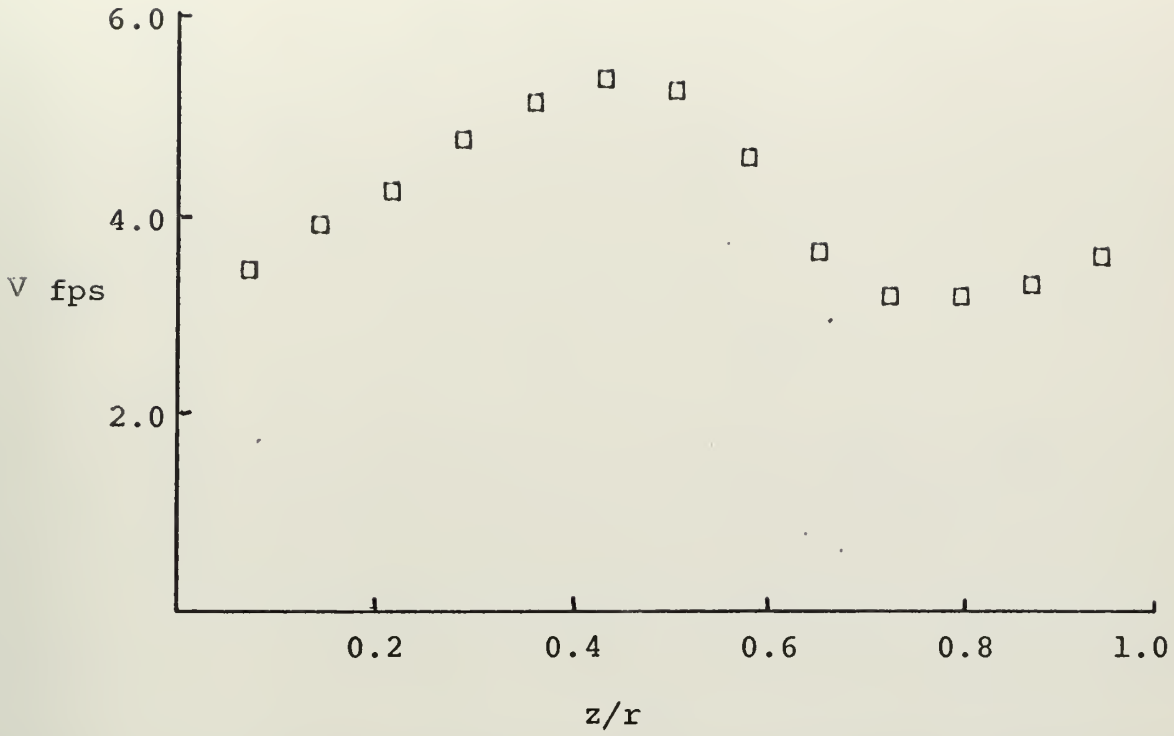

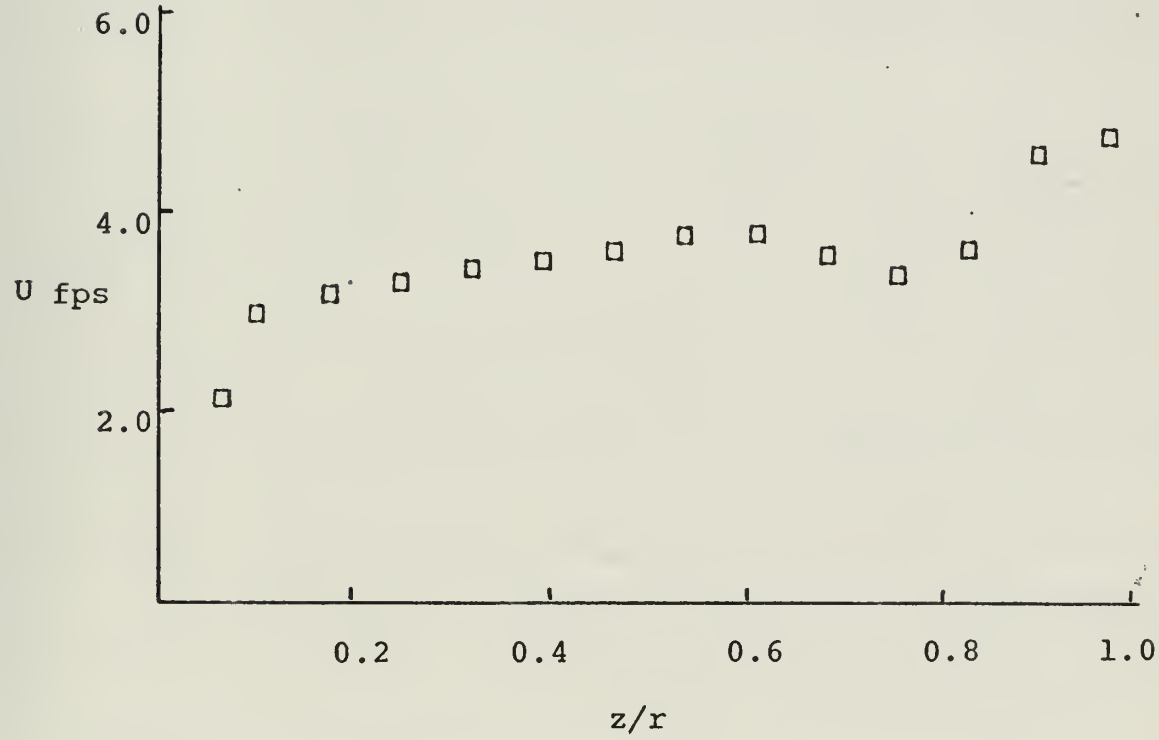

FIGURE 22. EXPERIMENTAL PROFILES. K=0.95 X=0.1

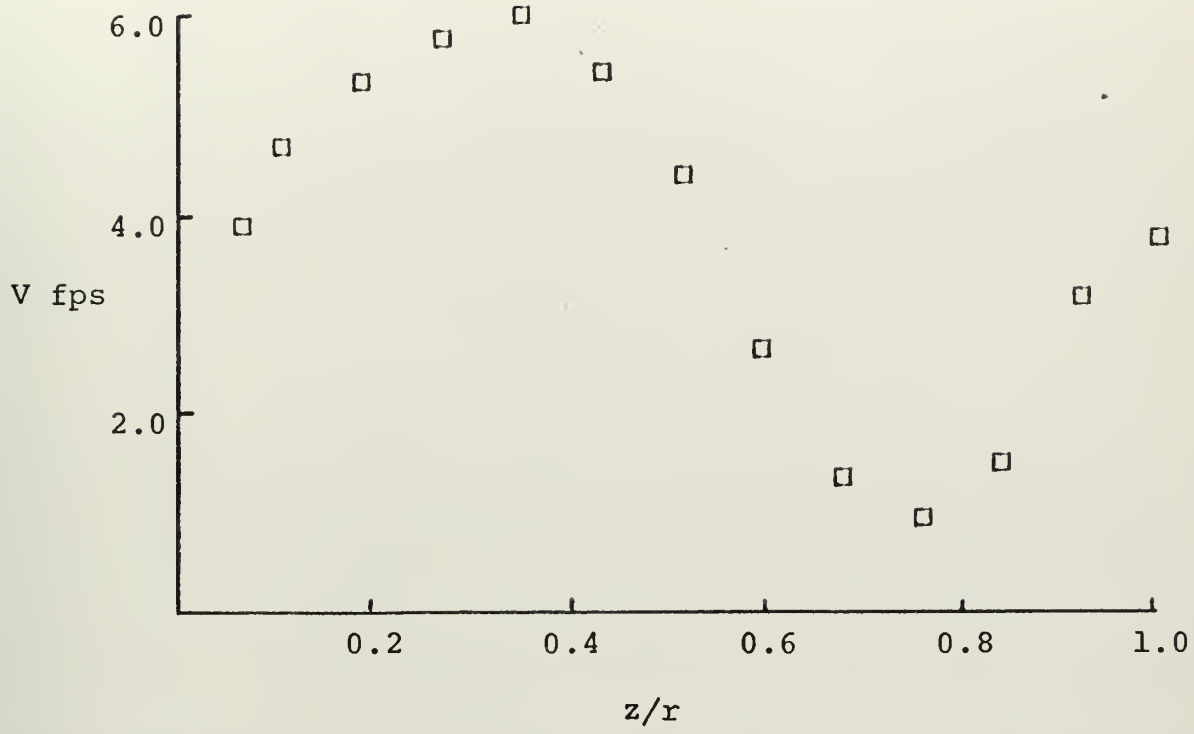

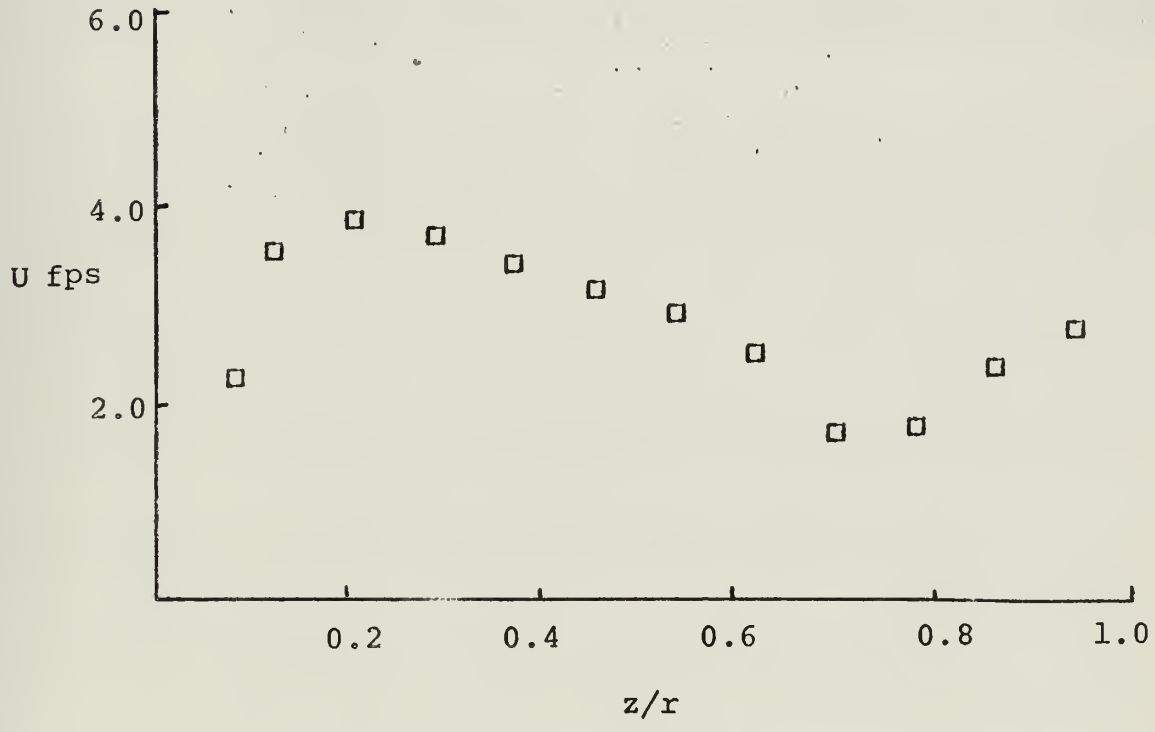

FIGURE 23. EXPERIMENTAL PROFILES. K=0.95 X+0.2

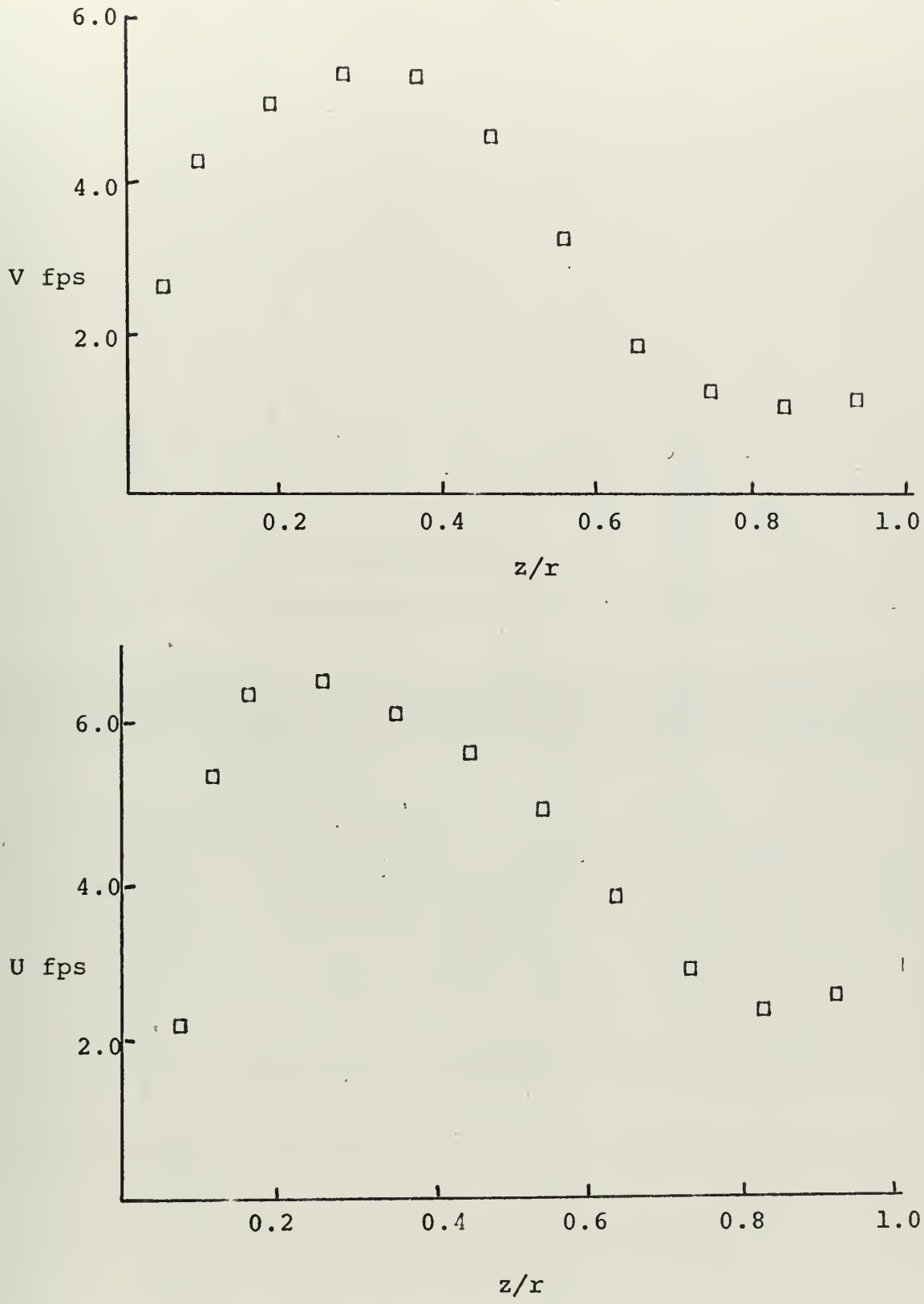

FIGURE 24. EXPERIMENTAL PROFILES. K=0.95 X=0.3

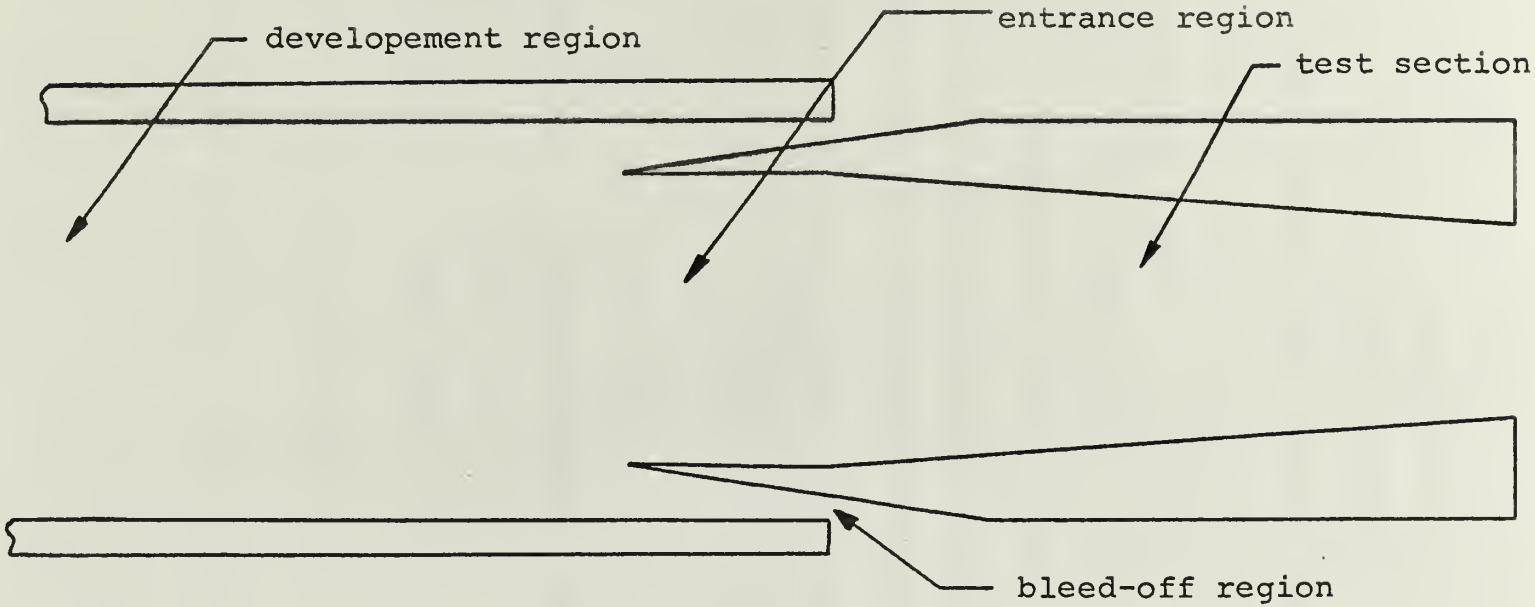

FIGURE 25. TEST SECTION CONFIGURATION.

IV. CONCLUSIONS AND RECOMMENDATIONS

Previous work in this area considered the effect of swirling flow upon the velocity profiles in the boundary layer. In this paper, the effect of the boundary layer growth upon the core velocities was utilized in the analysis. However, the experimental tests showed that this consideration was not enough. The swirl also affected the axial core flow, and the resultant changes are much more drastic than any variation in the boundary layer flow. Rather than applying the Navier-Stokes equations to the boundary layer alone, it would be much more appropriate to apply them to the whole flow field. In addition, the developed theory for the boundary layer assumed that a basically linear relationship existed between the various characteristic thicknesses. Since these thicknesses are functions of the shape factors, which are in turn functions of X, it would seem mandatory to extend this analysis without these assumptions of linear relationships. However, in order to complete such an analysis, more information needs to be known about the effect of swirl upon the core velocities.

APPENDIX A

DERIVATION OF EQUATIONS ACCORDING TO WILKS

The boundary of the convergent nozzle is formed by surface of revoltuion of a curve r(x), where x is a distance measured along the wall. The distance from the wall is z. The potential flow has the two components, V and U as shown below

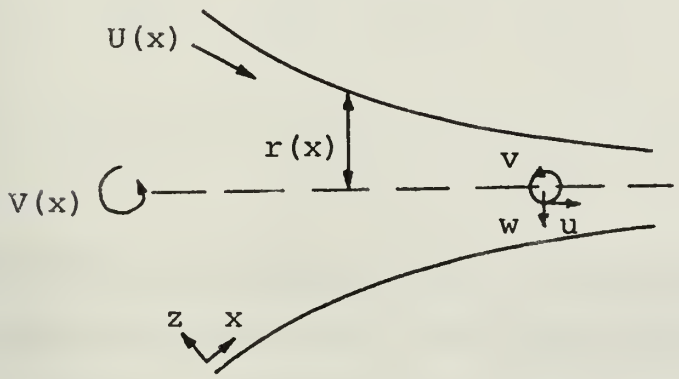

Acceleration in the orthogonal curvilinear coordinates is defined as

$$\vec{a} = \frac{D\vec{q}}{Dt} = \frac{\partial \vec{q}}{\partial t} + \nabla\,(1/2q^2) - \vec{q} \times \vec{\zeta}$$

In the $\vec{i}_i$ direction this becomes

$$\frac{\partial q_i}{\partial t} + \frac{q_1}{h_1}\frac{\partial q_i}{\partial u_1} + \frac{q_2}{h_2}\frac{\partial q_i}{\partial u_2} + \frac{q_3}{h_3}\frac{\partial q_i}{\partial u_3}$$

$$+ \frac{q_i}{h_i}\left\{ \frac{q_1}{h_1}\left(\frac{\partial h_i}{\partial u_1}\right) + \frac{q_2}{h_2}\left(\frac{\partial h_i}{\partial u_2}\right) + \frac{q_3}{h_3}\left(\frac{\partial h_i}{\partial u_3}\right)\right\}$$

$$- \frac{1}{h_i}\left\{ \frac{q_1^2}{h_1}\left(\frac{\partial h_1}{\partial u_i}\right) + \frac{q_2^2}{h_2}\left(\frac{\partial h_2}{\partial u_i}\right) + \frac{q_3^2}{h_3}\left(\frac{\partial h_3}{\partial u_i}\right)\right\}$$

If $u_1 = x$, $u_2 = \theta$, $u_3 = z$

$q_1 = u$, $q_2 = v$, $q_3 = w$

$h_1 = 1$, $h_2 = r$, $h_3 = 1$

the acceleration can be written

$$a_x = \frac{\partial u}{\partial t} + u \frac{\partial u}{\partial x} + \frac{v}{r} \frac{\partial u}{\partial \theta} + w \frac{\partial u}{\partial z} - \frac{v^2}{r} \frac{\partial r}{\partial x}$$

$$a_z = \frac{\partial w}{\partial t} + u \frac{\partial w}{\partial x} + \frac{v}{r} \frac{\partial w}{\partial \theta} + w \frac{\partial w}{\partial z} - \frac{v^2}{r} \frac{\partial r}{\partial z}$$

$$a_\theta = \frac{\partial v}{\partial t} + u \frac{\partial v}{\partial x} + \frac{v}{r} \frac{\partial v}{\partial \theta} + w \frac{\partial v}{\partial z} + \frac{v \cdot u}{r} \frac{\partial r}{\partial x}$$

For axisymmetric flow, all of the partial derivatives with respect to the angular displacement are zero. Since velocities in the direction perpendicular to the wall (the z direction) may be considered small compared to the other velocities, the momentum equation in the z direction may be neglected. By an order of magnitude analysis, the boundary-layer equations for steady laminar flow with constant properties become

$$u \frac{\partial u}{\partial x} + w \frac{\partial u}{\partial z} - \frac{v^2}{r} \frac{dr}{dx} = - \frac{1}{\rho} \frac{\partial P}{\partial x} + \nu^2 \frac{\partial^2 u}{\partial z^2}$$

$$u \frac{\partial v}{\partial x} + w \frac{\partial v}{\partial z} + \frac{uv}{r} \frac{dr}{dx} = - \frac{1}{\rho} \frac{\partial P}{\partial \theta} + \nu^2 \frac{\partial^2 v}{\partial z^2}$$

$$\frac{\partial}{\partial x} (r \cdot u) + \frac{\partial}{\partial z} (r \cdot w) = 0$$

with the boundary conditions

$u = v = 0$ on $z = 0$

$u \to U(x)$ and $v \to V(x) = A/r(x)$ as $z \to \infty$

With the above boundary conditions, the pressure gradient in the x-direction can then be written

$$-\frac{1}{\rho}\frac{\partial P}{\partial x} = U\frac{du}{dx} - V^2\frac{r'}{r}$$

Integrating the u-momentum equation across the boundary layer gives

$$\int_o^\infty \left(u\frac{\partial u}{\partial x} + w\frac{\partial u}{\partial z} - \frac{v^2}{r}\frac{dr}{dx} - U\frac{dU}{dx} + V^2\frac{r'}{r}\right)dz = -\nu\left(\frac{\partial u}{\partial z}\right)_o$$

from continuity

$$w = -\frac{1}{r}\int_o^z \frac{\partial}{\partial x}(r\cdot u)\,dz$$

Thus

$$\int_o^\infty \left(u\frac{\partial u}{\partial x} - \frac{1}{r}\frac{\partial u}{\partial z}\int_o^z \frac{\partial}{\partial x}(r\cdot u)\,dz - v^2\frac{r'}{r} - U\frac{dU}{dx} + V^2\frac{r'}{r}\right)dz = -\nu\left(\frac{\partial u}{\partial z}\right)_o$$

The second term

$$\int_o^\infty \frac{1}{r}\frac{\partial u}{\partial z}\int_o^z \frac{\partial}{\partial x}(r\cdot u)\,dz\,dz$$

can be integrated by parts.

$$m = \int_o^z \frac{\partial}{\partial x}(r\cdot u)\,dz \qquad dp = \frac{\partial u}{\partial z}\,dz$$

$$dm = \frac{\partial}{\partial x}(r\cdot u)\,dz \qquad p = u$$

$$m\,p\,\Big|_0^\infty - \int_0^\infty p\,dm = u\int_0^z \frac{\partial}{\partial x}(r\cdot u)\,dz\,\Big|_0^\infty - \int_0^\infty u\,\frac{\partial}{\partial x}(r\cdot u)\,dz$$

$$= U\int_0^\infty \frac{\partial}{\partial x}(r\cdot u)\,dz - \int_0^\infty u\,\frac{\partial}{\partial x}(r\cdot u)\,dz$$

The u momentum-integral equation then becomes

$$\int_0^\infty \left(u\,\frac{\partial u}{\partial x} - \frac{U}{r}\,\frac{\partial}{\partial x}(r\cdot u) + \frac{u}{r}\,\frac{\partial}{\partial x}(r\cdot u) - U\,\frac{dU}{dx}\right) dz$$

$$+ \int_0^\infty (V^2 - v^2)\,\frac{r'}{r}\,dz = -\nu\left(\frac{\partial u}{\partial z}\right)_0$$

The first integral can be written

$$\int_0^\infty \left(u\,\frac{\partial u}{\partial x} - \frac{U-u}{r}\cdot\left(r\,\frac{\partial u}{\partial x} + u\,\frac{\partial r}{\partial x}\right) - U\,\frac{dU}{dx}\right)\,dz$$

$$= \int_0^\infty \left(2\,u\,\frac{\partial u}{\partial x} - U\,\frac{\partial u}{\partial x} - \frac{(U-u)\cdot u}{r}\,\frac{dr}{dx} - U\,\frac{dU}{dx}\right) dz$$

Since

$$U\,\frac{\partial u}{\partial x} = \frac{\partial uU}{\partial x} - u\,\frac{dU}{dx}$$

the integral becomes

$$\int_0^\infty \left(\frac{\partial u^2}{\partial x} - \frac{\partial (uU)}{\partial x} + (u-U)\,\frac{dU}{dx} + \frac{(u-U)\cdot u}{r}\,\frac{dr}{dx}\right)\,dz$$

$$= \frac{1}{r}\,\frac{\partial}{\partial x}\left(r\int_0^\infty u\cdot(u-U)\,dz\right) + \frac{dU}{dx}\int_0^\infty (u-U)\,dz$$

The integral form of the v-momentum equation is

$$\int_0^\infty \left(u\,\frac{\partial v}{\partial x} + w\,\frac{\partial v}{\partial z} + \frac{u\cdot v}{r}\,\frac{dr}{dx}\right) dz = -\nu\left(\frac{\partial v}{\partial z}\right)_0$$

Introducing the continuity equation, this becomes

$$\int_0^\infty \left(u \frac{\partial v}{\partial x} - \frac{1}{r} \frac{\partial v}{\partial z} \int_0^\infty \frac{\partial}{\partial x} (r \cdot u)\, dz + \frac{u \cdot v}{r} \frac{dr}{dx} \right) dz = - \nu \left(\frac{\partial v}{\partial z} \right)_0$$

Performing an integration of the second term by parts

$$m = \int_0^z \frac{\partial}{\partial x} (r \cdot u)\, dz \qquad dp = \frac{1}{r} \frac{\partial v}{\partial z}\, dz$$

$$dm = \frac{\partial}{\partial x} (r \cdot u)\, dz \qquad p = \frac{v}{r}$$

$$m\, p \Big|_0^\infty - \int_0^\infty p\, dm = \int_0^\infty \frac{\partial}{\partial x} (r \cdot u)\, dz - \int_0^\infty \frac{v}{r} \frac{\partial}{\partial x} (r \cdot u)\, dz$$

The left hand side of the momentum-integral equation may now be written as

$$\int_0^\infty \left(u \frac{\partial v}{\partial x} - \frac{V}{r} \frac{\partial}{\partial x} (r \cdot u) + \frac{v}{r} \frac{\partial}{\partial x} (r \cdot u) + \frac{u \cdot v}{r} \frac{dr}{dx} \right) dz$$

$$= \int_0^\infty \left[\left(\frac{\partial (v \cdot u)}{\partial x} - v \frac{\partial u}{\partial x} \right) - V \frac{\partial u}{\partial x} + v \frac{\partial u}{\partial x} - \frac{(V-v)}{r} u \frac{\partial r}{\partial x} + \frac{v \cdot u}{r} \frac{dr}{dx} \right] dz$$

$$= \int_0^\infty \left(\frac{\partial}{\partial x} (v \cdot u) - V \frac{\partial u}{\partial x} - \frac{V \cdot u}{r} \frac{\partial r}{\partial x} + \frac{2 \cdot u \cdot v}{r} \frac{dr}{dx} \right) dz$$

Since

$$V \frac{\partial u}{\partial x} = \frac{\partial}{\partial x} (V \cdot u) - u \frac{dV}{dx} = \frac{\partial}{\partial x} (V \cdot u) + \frac{u \cdot V}{r} \frac{dr}{dx}$$

the equation can be written

$$\int_0^\infty \left(\frac{\partial}{\partial x} (v \cdot u - V \cdot u) + \frac{2 \cdot u}{r} (v - V) \frac{dr}{dx} \right) dz = - \nu \left(\frac{\partial v}{\partial z} \right)_0$$

Thus the v momentum-integral equation is

$$\frac{1}{r^2}\frac{d}{dx}\left(r^2 \int_o^\infty u\,(v-V)\,dz \right) = -\nu \left(\frac{\partial v}{\partial z}\right)_o$$

with the boundary conditions

$$\left.\begin{aligned} v &= 0 \\ \frac{\partial^2 v}{\partial z^2} &= 0 \end{aligned}\right\} \text{on} \quad z = 0$$

$$\left.\begin{aligned} v &= V(x) = \frac{A}{r(x)} \\ \frac{\partial v}{\partial z} &= 0 \\ \frac{\partial^2 v}{\partial z^2} &= 0 \end{aligned}\right\} \text{when } z \to \infty$$

The u momentum-integral equation is

$$\frac{1}{r}\frac{d}{dx}\left(r \int_o^\infty u\,(u-U)\,dz \right) + \frac{dU}{dx}\int_o^\infty (u-U)\,dz + \frac{1}{r}\frac{dr}{dx}\int_o^\infty (V^2-v^2)\,dz = -\nu\left(\frac{\partial u}{\partial z}\right)_o$$

with the boundary conditions

$$\left.\begin{aligned} u &= 0 \\ -\nu\frac{\partial^2 u}{\partial z^2} &= U\frac{dU}{dx} - \frac{V^2}{r}\frac{dr}{dx} \end{aligned}\right\} \text{on} \quad z = 0$$

$$\left.\begin{aligned} u &= U(x) \\ \frac{\partial u}{\partial z} &= 0 \\ \frac{\partial^2 u}{\partial z^2} &= 0 \end{aligned}\right\} \text{ when } z \to \infty$$

In order to obtain a solution to the momentum-integral equations using the approximate method of von Karman, it is necessary to assume suitable velocity profiles. A direct analogy with the Pohlhausen method would lead to

$$u/U = f(n,L_1) \qquad v/V = g(n,L_2)$$

where $n = z/\delta(x)$. The continuity equation leads to a stream function

$$\psi = r \cdot U \cdot h(x,n)$$

The axial velocity can then be written

$$u = U \frac{\partial}{\partial n} h(x,n)$$

If the tangential velocity is of the form $v = V \cdot g(x,n)$, the momentum equations may be written

$$h''' + a \cdot h \cdot h'' + b \cdot (1-h'^2) + d \cdot (1-g^2) = 0$$

$$g'' + a \cdot h \cdot g' = 0$$

where a, b, and d are constants as defined by Wilks. Boundary conditions require that g" evaluated at the wall is zero. A differentiated form of the v-momentum equation gives

$$g''' + a \cdot (h' \cdot g' + h \cdot g'') = 0$$

Since both h' and g" evaluated at the wall are zero, it is apparent the g"' evaluated at n = 0 must also be zero. This would require the second and third derivatives of g to be

independent of x. With this understanding, the two parameters can be used to obtain the axial velocity profile while the tangential profile is considered dependent upon n alone. Thus

$$u/U = f(n,L_1,L_2) \quad \text{and} \quad v/V = g(n)$$

Introducing a dimensionless length X=x/c (c being the length of the cone along the generator), the u momentum-integral equation becomes

$$\frac{1}{c\cdot r}\frac{d}{dX}\left(r\cdot U^2\cdot\delta \int_o^1 f(f-1)\,dn\right) + \frac{1}{c}\frac{dU}{dX}\,U\cdot\delta\int_o^1 (f-1)\,dn + \frac{1}{c\cdot r}V^2\frac{dr}{dX}\cdot\delta\int_o^1 (1-g^2)\,dn = -\nu\frac{U}{\delta}f'(0)$$

with the boundary conditions

$$\left.\begin{aligned} f &= 0 \\ -\frac{\nu U}{\delta^2}f'' &= \frac{U}{c}\frac{dU}{dX} - \frac{V^2}{c\cdot r}\frac{dr}{dX}\end{aligned}\right\} \text{ on } n = 0$$

$$\left.\begin{aligned} f &= 1 \\ f' &= 0 \\ f''' &= 0\end{aligned}\right\} \text{ on } n = 1$$

The v momentum-integral becomes

$$\frac{1}{c\cdot r^2}\frac{d}{dX}\left(r^2\cdot U\cdot V\cdot\delta\int_o^1 f(1-g)\,dn\right) = \frac{\nu}{\delta}V\cdot g'(0)$$

with the boundary conditions

$$\left.\begin{aligned} g &= 0 \\ g'' &= 0\end{aligned}\right\} \text{ on } n = 0$$

$$\left.\begin{aligned} g &= 1 \\ g' &= 0 \\ g'' &= 0 \end{aligned}\right\} \text{ on } n = 1$$

Here it was assumed that the boundary conditions could be transferred from infinity to the boundary-layer thickness, that is where n=1, without appreciable error.

In an attempt to obtain an improvement in the basic approximate method of solution, a profile can be obtained that will also satisfy the requirements of the energy-integral equation. Weighardt [3] developed such a method using two-parameter profiles. This profile can be represented with the aid of an eleventh order polynomial. Thus

$$u/U = f_1(n) + L_1 \cdot f_2(n) + L_2 \cdot f_3(n)$$

where

$$f_1(n) = 1 - (1-n)^8(1 + 8n + 36n^2 + 120n^3)$$

$$f_2(n) = (1-n)^8 n\,(1 + 8n + 36n^2)$$

$$f_3(n) = -(1-n)^8 n^2(1 + 8n)$$

Evaluating the functions at the wall (n=0) yields

$$\mu\left(\frac{\partial u}{\partial z}\right)_o = \frac{\mu U}{\delta}\left(\frac{\partial f}{\partial n}\right)_o = \frac{\mu U}{\delta} L_1$$

thus

$$L_1 = \frac{\delta \tau_o}{\mu U}$$

Also

$$-\frac{\nu U}{\delta^2} f'' = \frac{U}{c}\frac{dU}{dX} - \frac{V^2}{c \cdot r}\frac{dr}{dX} \quad \text{at} \quad n=0$$

where $f''(0) = -2\ L_2$

This leads to

$$L_2 = \frac{U\delta}{\nu}\frac{\delta}{2c}\left[\frac{U'}{U} - \left(\frac{V}{U}\right)^2 \frac{r'}{r}\right]$$

The integrals in the momentum integral equations can be expressed as various characteristic thicknesses.

$$\delta_{1x} = \delta \int_o^1 (1-f)\,dn$$ displacement thickness in the x direction

$$\delta_{2x} = \delta \int_o^1 f(1-f)\,dn$$ momentum thickness in the x direction

$$\delta_{2xy} = \delta \int_o^1 (1-g)\,dn$$ mixed momentum thickness

With the definition of a new thickness

$$\delta_4 = \delta \int_o^1 (1-g^2)\,dn$$

the momentum-integral equations can now be written

$$\frac{1}{c \cdot r}\frac{d}{dX}(r \cdot U^2 \cdot \delta_{2x}) + \frac{1}{c}\frac{dU}{dX} U\ \delta_{1x} - \frac{1}{c \cdot r} V^2 \frac{dr}{dX}\delta_4 = \nu \frac{U}{\delta} f'(0)$$

$$\frac{1}{c \cdot r}\frac{d}{dX}(r^2 \cdot U \cdot V \cdot \delta_{2xy}) = \frac{\nu}{\delta} V\ g'(0)$$

Differentiating the appropriate terms, these equations simplify to

$$\frac{r'}{r} + \frac{U'}{U}(2 + A1) + \frac{\delta'_{2x}}{\delta_{2x}} = \frac{\nu c}{U \cdot \delta^2} A2 + \frac{r'}{r}\frac{V^2}{U^2} A3$$

$$\frac{r'}{r} + \frac{U'}{U} + \frac{\delta'_{2xy}}{\delta_{2xy}} = \frac{\nu c}{U \cdot \delta^2} A4$$

where

$$A1 = \frac{\int_o^1 (1-f)\,dn}{\int_o^1 f(1-f)\,dn} = \frac{\delta_{1x}}{\delta_{2x}} = \frac{D1}{D2}$$

$$A2 = \frac{f'(0)}{\int_o^1 f(1-f)\,dn} = \frac{L_1}{D2}$$

$$A3 = \frac{\int_o^1 (1-g^2)\,dn}{\int_o^1 f(1-f)\,dn} = \frac{D4}{D2}$$

$$A4 = \frac{g''(0)}{\int_o^1 f(1-g)\,dn} = \frac{2}{D3}$$

An integration of the polynomials in the above integrals led to

$$D1 = 0.3333333 - 0.0454545\ L_1 + 0.006060\ L_2$$

$$D2 = 0.0740342 + 0.0149190\ L_1 - 0.00118583\ L_2$$

$$- 0.0045481\ L_1^2 - 0.00008286\ L_2^2 + 0.0012013\ L_1 L_2$$

$$D3 = 0.08461538 + 0.02435846\ L_1 - 0.00293040\ L_2$$

$$D4 = 0.4174603$$

Wilks made the assumption that a basically linear relationship existed between the boundary-layer thickness and the momentum thickness. This assumes that D2 does not vary significantly with X. A basically linear relationship between the mixed-momentum thickness and the boundary-layer thickness was also assumed.

With the introduction of a dimensionless parameter

$$G = \frac{U\delta}{\nu}\frac{\delta}{c}$$

the foregoing equations can now be written

$$\frac{r'}{r} + \frac{U'}{U}(2 + A1) + \frac{\delta'}{\delta} = \frac{A2}{G} + \frac{r'}{r}\left(\frac{V}{U}\right)^2 A3$$

$$\frac{r'}{r} + \frac{U'}{U} + \frac{\delta'}{\delta} = \frac{A4}{G}$$

Now

$$\frac{G'}{G} = 2\frac{\delta'}{\delta} + \frac{U'}{U}$$

Combining these three equations yields

$$G' = 2\ A4 - \frac{(A2 - A4)}{(A1 + 1)} - G\frac{r'}{r}\left[2 + \left(\frac{V}{U}\right)^2 \frac{A3}{(1 + A1)}\right]$$

$$A2 = G\frac{U'}{U}(1 + A1) + A4 - G\frac{r'}{r}\left(\frac{V}{U}\right)^2 A3$$

In addition to the above relationships, the previously derived equation for the shape factor L_2 is also important, viz.,

$$L_2 = \frac{G}{2}\left[\frac{U'}{U} - \left(\frac{V}{U}\right)^2 \frac{r'}{r}\right]$$

The following characteristics must be considered for the perfectly conical nozzle.

$$r(X) = r_o(1 - X)$$

By continuity

$$U_o \cdot r_o^2 \cdot \pi = U(X)\, r_o^2 \cdot (1 - X)^2 \cdot \pi$$

$$U(X) = \frac{U_o}{(1 - X)^2}$$

Conservation of angular momentum requires that

$$V_o \cdot r_o = V(X) \cdot r_o \cdot (1 - X) = A$$

If $V_o = K \cdot U_o$

$$V(X) = \frac{K \cdot U_o}{(1 - X)}$$

Furthermore,

$$\frac{U'}{U} = \frac{2}{(1 - X)}$$

and

$$\frac{r'}{r} = \frac{-1}{(1 - X)}$$

APPENDIX B

DERIVATION OF PRESENT THEORY

The concept of a free vortex in the inviscid core requires that the tangential velocity be inversely proportional to the radius. In the case where boundary layer growth is large, the boundary layer thickness can no longer be considered thin in comparison to the radius. With these considerations, the boundary conditions for the momentum equation become

$$v \to V(x) = A/(r-\delta) \quad \text{as} \quad z \to \infty$$

This new definition of V(x) has no effect upon the development of the u momentum-integral equation. However, there is an effect in the v momentum-integral equation. The development is the same as described in Appendix A up to the point

$$\int_0^\infty \left(\frac{\partial (vu)}{\partial x} - V\frac{\partial u}{\partial x} - \frac{V \cdot u}{r}\frac{dr}{dx} + \frac{2 \cdot u \cdot v}{r}\frac{dr}{dx} \right) dz = -\nu \left(\frac{\partial v}{\partial z} \right)_o$$

Now

$$V\frac{\partial u}{\partial x} = \frac{\partial (Vu)}{\partial x} - u\frac{\partial V}{\partial x}$$

$$= \frac{\partial (Vu)}{\partial x} + \frac{u \cdot V}{r-\delta} \cdot \left(\frac{dr}{dx} - \frac{d\delta}{dx} \right)$$

Thus the momentum-integral equation becomes

$$\int_o^\infty \left[\frac{\partial}{\partial x}(vu - Vu) + \frac{2 \cdot u}{r} \cdot (v - V)\frac{dr}{dx} + \frac{u \cdot V}{r}\frac{dr}{dx} + \frac{u \cdot V}{r-\delta}\left(\frac{d\delta}{dx} - \frac{dr}{dx} \right) \right] dz$$

$$= -\nu \left(\frac{\partial v}{\partial z} \right)_o$$

Simplifing

$$\frac{1}{r^2}\frac{d}{dx}\left(r^2\int_o^\infty u(v-V)\,dz\right) + \frac{V}{r-\delta}\left(\frac{d\delta}{dx} - \frac{\delta}{r}\frac{dr}{dx}\right)\int_o^\infty u\cdot dz = -\nu\left(\frac{\partial v}{\partial z}\right)_o$$

Introducing the velocity profiles as in Appendix A, the momentum-integral equations and the appropriate boundary conditions become

$$\frac{1}{c\cdot r}\frac{d}{dX}\left(r\cdot U^2\cdot\delta\int_o^1 f(f-1)\cdot dn\right) + \frac{1}{c}\cdot\frac{dU}{dX}\cdot U\cdot\delta\cdot\int_o^1 (f-1)\cdot dn$$

$$+ \frac{1}{c\cdot r}\cdot V^2\cdot\frac{dr}{dX}\cdot\delta\cdot\int_o^1 (1-g^2)\,dn = -\nu\frac{U}{\delta}\cdot f'(0)$$

with the boundary conditions

$$\left.\begin{aligned} &\text{(i)} && f = 0 \\ &\text{(ii)} && -\frac{\nu U}{\delta^2}f'' = \frac{U}{c}\cdot\frac{dU}{d} - \frac{V^2}{c\cdot r}\frac{dr}{d} \end{aligned}\right\} \text{on} \quad n = 0$$

$$\left.\begin{aligned} &\text{(iii)} && f = 1 \\ &\text{(iv)} && f' = 0 \\ &\text{(v)} && f'' = 0 \end{aligned}\right\} \text{on} \quad n = 1$$

and

$$\frac{1}{cr^2}\frac{d}{dX}\left(r^2\cdot U\cdot V\cdot\delta\cdot\int_o^1 f(1-g)\,dn\right) + \frac{U\cdot V}{r-\delta}\cdot\frac{1}{c}\left(\frac{d\delta}{dX} - \frac{\delta}{r}\frac{dr}{dX}\right)\delta\int_o^1 f\,dn$$

$$= -\frac{\nu A}{\delta r}g'(0)$$

with the boundary conditions

$$\left.\begin{aligned} &\text{(i)} && g = 0 \\ &\text{(ii)} && g'' = 0 \end{aligned}\right\} \text{on} \quad n = 0$$

$$\left.\begin{array}{ll} \text{(iii)} & g = 1 \\ \text{(iv)} & g' = 0 \\ \text{(v)} & g'' = 0 \end{array}\right\} \text{on} \quad n = 0$$

Again, it was assumed that a basically linear relationship existed between the boundary-layer thickness and both the momentum and mixed-momentum thicknesses. Defining the coefficients A1, A2, A3, and A4 as in Appendix A, and introducing a new term

$$A5 = \frac{\int_0^1 f\, dn}{\int_0^1 f(1-g)\, dn} = \frac{1 - D1}{D3}$$

the momentum-integral equations then became

$$\frac{r'}{r} + \frac{U'}{U}(2 + A1) + \frac{\delta'}{\delta} = \frac{A2}{G} + \frac{r'}{r}\cdot\left(\frac{V}{U}\right)^2 \cdot A3$$

$$\frac{2r'}{r} + \frac{U'}{U} + \frac{V'}{V} + \frac{\delta'}{\delta} + \frac{1}{r/\delta - 1}\left(\frac{\delta'}{\delta} - \frac{r'}{r}\right)\cdot A5 = \frac{A4}{G}$$

The second equation can be rewritten

$$\frac{\delta'}{\delta} = \left[\frac{A4}{G} - \frac{U'}{U} - \frac{V'}{V} - \frac{r'}{r}\left(2 - \frac{A5}{r/\delta - 1}\right)\right] / \left(1 + \frac{A5}{r/\delta - 1}\right)$$

Thus, the shape factor L_1 can be obtained from

$$A2 = G\left[\frac{U'}{U}\cdot(2 + A1) + \frac{r'}{r}\cdot\left(1 - \frac{V^2}{U^2} A3\right) + \frac{\delta'}{\delta}\right]$$

and the new values for G and L_2 can be calculated from the value of G', where G' is now

$$G' = G\cdot\left(2\,\frac{\delta'}{\delta} + \frac{U'}{U}\right)$$

and

$$L_2 = \frac{G}{2}\left[\frac{U'}{U} - \left(\frac{V}{U}\right)^2 \frac{r'}{r}\right]$$

As the boundary layer grows, the axial velocity as defined in APPENDIX A for a cone will no longer be valid. The increasing boundary-layer thickness will cause the flow in the axial direction to accelerate more than would be caused by the convergence of the cone alone. The concept of displacement thickness would take into consideration this change in the effective radius of the cone. Continuity now yields

$$U_o \cdot \left[r_o - \delta_{1x}(0)\right]^2 \cdot \pi = U(X) \cdot \left[r_o \cdot (1-X) - \delta_{1x}(X)\right]^2 \cdot \pi$$

thus

$$U(X) = \frac{U_o \cdot \left[1 - \frac{\delta_{1x}(0)}{r_o}\right]^2}{\left[(1-X) - \frac{\delta_{1x}(X)}{r_o}\right]^2}$$

and

$$\frac{U'}{U} = \frac{2 \cdot \left[1 + \frac{\delta'_{1x}(X)}{r_o}\right]}{(1-X) - \frac{\delta_{1x}(X)}{r_o}}$$

With the new definition of V(X), the conservation of angular momentum yields

$$V_o \cdot r_o - \delta(0) = V(X) \cdot r_o \cdot (1-X) - \delta(X)$$

$$V(X) = \frac{K \cdot U_o \cdot \left[1 - \frac{\delta(0)}{r_o}\right]}{(1-X) - \frac{\delta(X)}{r_o}}$$

BIBLIOGRAPHY

1. Taylor, G. I., "The Boundary Layer in the Converging Nozzle of a Swirl Atomizer," Quarterly Journal of Mechanics and Applied Mathematics, Vol. III, Part 2, p. 129-140, 1950.

2. Wilks, Graham, "Swirling Flow in a Convergent Funnel," Journal of Fluid Mechanics, Vol. 34, p. 575-593, 1968.

3. Aeronautical Research Council Report 9825, On an Energy Equation for the Calculation of the Laminar Boundary Layers, by K. Weighardt, 1946.

4. Lay, J. E., "An Experimental and Analytical Study of Vortex-Flow Temperature Separation of Spiral and Axial Flow, Part 1," Journal of Heat Transfer, p. 205-212, 1950.

INITIAL DISTRIBUTION LIST

		No. Copies
1.	Defense Documentation Center Cameron Station Alexandria, Virginia 22314	2
2.	Library, Code 0212 Naval Postgraduate School Monterey, California 93940	2
3.	Asst. Professor T. M. Houlihan, Code 59 Department of Mechanical Engineering Naval Postgraduate School Monterey, California 93940	1
4.	LT(j.g.) Douglas J. Hornstra, USN 390 Central Street East Bridgewater, Massachusetts 02333	1
5.	Professor T. Sarpkaya, Code 59 Department of Mechanical Engineering Naval Postgraduate School Monterey, California 93940	1

Security Classification

DOCUMENT CONTROL DATA - R & D

(Security classification of title, body of abstract and indexing annotation must be entered when the overall report is classified)

1 ORIGINATING ACTIVITY (Corporate author)

Naval Postgraduate School
Monterey, California 93940

2a. REPORT SECURITY CLASSIFICATION

Unclassified

2b. GROUP

3 REPORT TITLE

An Investigation of Swirling Flow In a Convergent Funnel

4. DESCRIPTIVE NOTES (Type of report and inclusive dates)

Master's Thesis; June 1970

5. AUTHOR(S) (First name, middle initial, last name)

Douglas John Hornstra

6. REPORT DATE	7a. TOTAL NO. OF PAGES	7b. NO. OF REFS
June 1970	75	4

8a. CONTRACT OR GRANT NO.	9a. ORIGINATOR'S REPORT NUMBER(S)
b. PROJECT NO.	
c.	9b. OTHER REPORT NO(S) (Any other numbers that may be assigned this report)
d.	

10. DISTRIBUTION STATEMENT

This document has been approved for public release and sale; its distribution is unlimited.

11. SUPPLEMENTARY NOTES	12. SPONSORING MILITARY ACTIVITY
	Naval Postgraduate School Monterey, California 93940

13. ABSTRACT

The boundary layer for a swirling flow of incompressible fluid in a convergent cone has been investigated. Theoretical calculations with boundary conditions more appropriate to physically existent situations discount the existence of "super velocities" within the boundary layer. Parallel experimental investigations demonstrate an interdependence of core and boundary layer flows which precludes the maintenance of initial "ideal flow" condtions.

DD FORM 1 NOV 65 1473 (PAGE 1)

S/N 0101-807-6811

Security Classification

A-31408

KEY WORDS	LINK A		LINK B		LINK C	
	ROLE	WT	ROLE	WT	ROLE	WT
Swirling Flow						
Convergent Funnel						

Thesis
H8037 Hornstra
c.1 An investigation of swirling flow in a convergent funnel.
120255